2020

DEVELOPMENT OF MICRO-SCALE HIGH ASPECT RATIO PATTERNED FEATURES WITH ELECTROLESS NICKEL PLATING

Lorli Smith
University of Kentucky, lorli.smith@yahoo.com
Digital Object Identifier: https://doi.org/10.13023/etd.2020.457

STUDENT AGREEMENT:

I represent that my thesis or dissertation and abstract are my original work. Proper attribution has been given to all outside sources. I understand that I am solely responsible for obtaining any needed copyright permissions. I have obtained needed written permission statement(s) from the owner(s) of each third-party copyrighted matter to be included in my work, allowing electronic distribution (if such use is not permitted by the fair use doctrine) which will be submitted to UKnowledge as Additional File.

I hereby grant to The University of Kentucky and its agents the irrevocable, non-exclusive, and royalty-free license to archive and make accessible my work in whole or in part in all forms of media, now or hereafter known. I agree that the document mentioned above may be made available immediately for worldwide access unless an embargo applies.

I retain all other ownership rights to the copyright of my work. I also retain the right to use in future works (such as articles or books) all or part of my work. I understand that I am free to register the copyright to my work.

REVIEW, APPROVAL AND ACCEPTANCE

The document mentioned above has been reviewed and accepted by the student's advisor, on behalf of the advisory committee, and by the Director of Graduate Studies (DGS), on behalf of the program; we verify that this is the final, approved version of the student's thesis including all changes required by the advisory committee. The undersigned agree to abide by the statements above.

Lorli Smith, Student

Dr. Christine Trinkle, Major Professor

Dr. Alexandre Martin, Director of Graduate Studies

DEVELOPMENT OF MICRO-SCALE HIGH ASPECT RATIO PATTERNED FEATURES WITH ELECTROLESS NICKEL PLATING

THESIS

A thesis submitted in partial fulfillment of the requirements for the degree of Master of Science in Mechanical Engineering in the College of Engineering at the University of Kentucky

By

Lorli Smith

Lexington, KY

Director: Dr. Christine Trinkle, Professor of Mechanical Engineering

Lexington, KY

2020

ABSTRACT

DEVELOPMENT OF MICRO-SCALE HIGH ASPECT RATIO PATTERNED FEATURES WITH ELECTROLESS NICKEL PLATING

This thesis describes a novel method designed to pattern high aspect ratio metallic microscale features using a modified photolithography and electroless nickel plating process. This method utilizes modified photolithography techniques to create a polymer mold that is used to control the location of metal deposition on substrate during electroless nickel plating. In order to generate high aspect ratio mold features, a multiple spin-step process was developed to deposit thick layers of SU-8 photoresist, and inclined lithography was also used to generate tapered sidewalls that could help aid mold removal after plating. Results from electroplating experiments were evaluated using a Zygo interferometer and cast PDMS mold cross-sections to determine plating thickness and uniformity.

KEYWORDS: MEMS, Microscale Manufacturing, Electroless Nickel Plating Applications, Inclined Lithography, High-Aspect Ratio Photolithography

Lorli Smith

_____

(Authorized Signature)

November 8, 2020

_____

(Date)

DEVELOPMENT OF MICRO-SCALE HIGH ASPECT RATIO PATTERNED FEATURES WITH ELECTROLESS NICKEL PLATING

By

Lorli Smith

Dr. Christine Trinkle

_____

Director of Thesis

Dr. Alexandre Martin

_____

Director of Graduate Studies

November 8, 2020

_____

Date

ACKNOWLEDGEMENTS

The following thesis, could not have been accomplished without the insights and direction of several people. First, I would like to thank my Thesis Chair, Dr. Christine Trinkle, who provided support, patience and exemplary guidance. In addition, Dr. Trinkle provided timely and instructive comments and evaluation at every stage of the thesis process. Next, I wish to thank my Thesis Committee, Dr. Sean Bailey and Dr. Brad Berron. Each individual provided insights that guided and challenged my thinking, substantially improving the finished product.

Table of Contents

List of Tables

List of Figures

Chapter 1 Introduction

The need for metallic molds with micro-scale patterned features is growing as fields such as microfluidics become more popular. But these molds can be challenging to make, especially when they involve high aspect ratio features in size ranges between the standard available machining sizes (larger than a few millimeters) and those of traditional micro-manufacturing techniques (smaller than 50 μm). Many methods for producing such geometry are commercially available however, manufacturing these features typically requires expensive materials and equipment and long lead times, making it inaccessible for many applications.

This thesis describes a novel microfabrication technique that relies on a combination of photolithography and electroless nickel plating. Photolithography is used to create a solid pattern in a photosensitive material called a photoresist. This pattern can then be used as a mold: when pressed against a metal substrate and submerged in an electroless nickel plating solution, the surface of the metal substrate is plated around the photoresist mold, creating plated features that are the inverse of the mold geometry. This methodology offers a cost and time efficient option to create metallic molds for manufacturing applications like injection molding.

The chapters of this thesis describe the development of this protocol, implementation through integrated experimentation, and results of each module. Chapter 2 presents and overview of the micropatterning method developed in this thesis, as well as a review of the literature covering other metal microfabrication methods. Chapter 3 discusses the methods used to create high-aspect ratio SU-8 features. This protocol is necessary in order to create the desired patterned mold that will be used in the electroless nickel plating process. Chapter 4 details the process used to generate tapered sidewall features in SU-8 using inclined photolithography. The tapered sidewalls aided in the mold release discussed in Chapter 5. Chapter 5 describes the electroless plating protocol used to generate plated high aspect ratio features by using samples with features generated from Chapter 3 as a mold.

Chapter 2 Background and Project Overview

In this study, a protocol was developed with the goal of easing the cost of manufacturing patterned high aspect ratio metallic microscale features, by using a modified photolithography and electroless nickel plating. Using modified photolithography techniques, a mold made from a photopolymer called SU-8 is used to plate a metallic substrate via electroless nickel plating (ENP). The substrate is plated in the exposed regions of metal around the mold, creating the inverse features. This methodology was developed as an alternative to traditional machining methods for ease of access, quick lead time, and cost efficiency. This chapter will discuss some of the alternative methods for creating these types of microscale features, in contrast with the molding/ENP method developed in this thesis.

2.1 Metal Micropattering Techniques

Numerous methods exist to create patterns of metal on the microscale. Some "additive" methods deposit layers of metal in a pattern on a surface, like evaporation and sputtering. While "subtractive" methods like wire EDM and traditional milling start with a bulk piece of material and carefully remove segments to develop a pattern.

2.1.1 Evaporation

Evaporation is a method of deposition that uses heat to evaporate a material such that the vaporized atoms travel to and are deposited on the desired substrate surface. This method is typically used to apply films or coatings to surfaces. The source or target material can be liquid or solid, and when a pure metallic is used as the target material, the vaporized particle is the atomic form of this metal [1]. This is known as direct evaporation, where the material vaporized is the same material that is deposited. This is performed in a vacuum. Figure 2.1 illustrates this process.

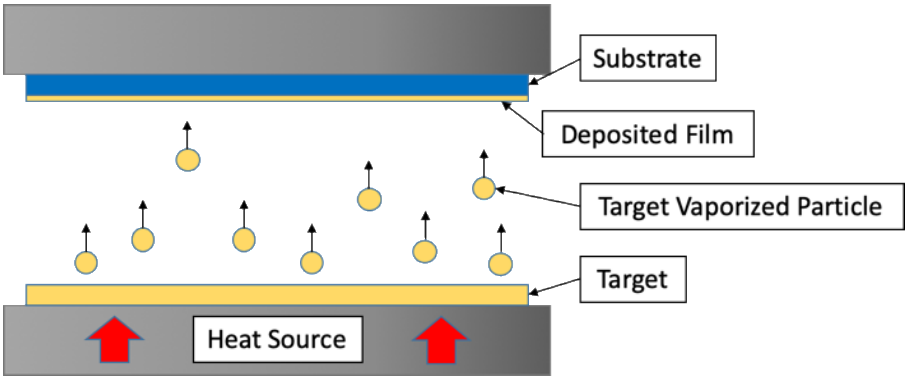

Figure 2.1 Evaporation Process

To create a layer of oxidized metal, such as silicon dioxide or aluminum oxide, small amounts of oxygen are introduced to the system in which the ion of the target material reacts with the ambient oxygen and deposits onto the substrate as the oxidized form of the target material. This is known as reactive evaporation [2].

This method is capable of producing very pure films of material, however the deposition rate is relatively low—typically 10-100 nm per minute. For the type of features needed in this thesis (250 µm height), it would take 42-420 hours to evaporate the necessary material. Therefore, because of the low deposition rate evaporation provides, this technology is not a viable option to investigate for this study.

2.1.2 Sputtering

Sputtering offers a potential deposition technique as well. Sputtering is a process in which a thin layer of atoms of a metal are deposited onto a surface in a vacuum [3]. An electric voltage is applied between the anode and the cathode of the system, energizing the gas in between the two, generating ionized gas molecules (plasma) that are propelled towards the target (cathode). These molecules collide with the target, and the transferred energy causes atoms to dislodge from the target surface. The dislodged atoms travel towards the surface of the anode at such high speed that when they hit the surface, they become adhered to the substrate or sputtered film surface. This occurs in a vacuum while circulating a controlled pressure between 0.1-0.5 Pa of either inert surrounding gas or a mixture of an inert gas and a reactive gas [3]. Figure 2.2 illustrates this process.

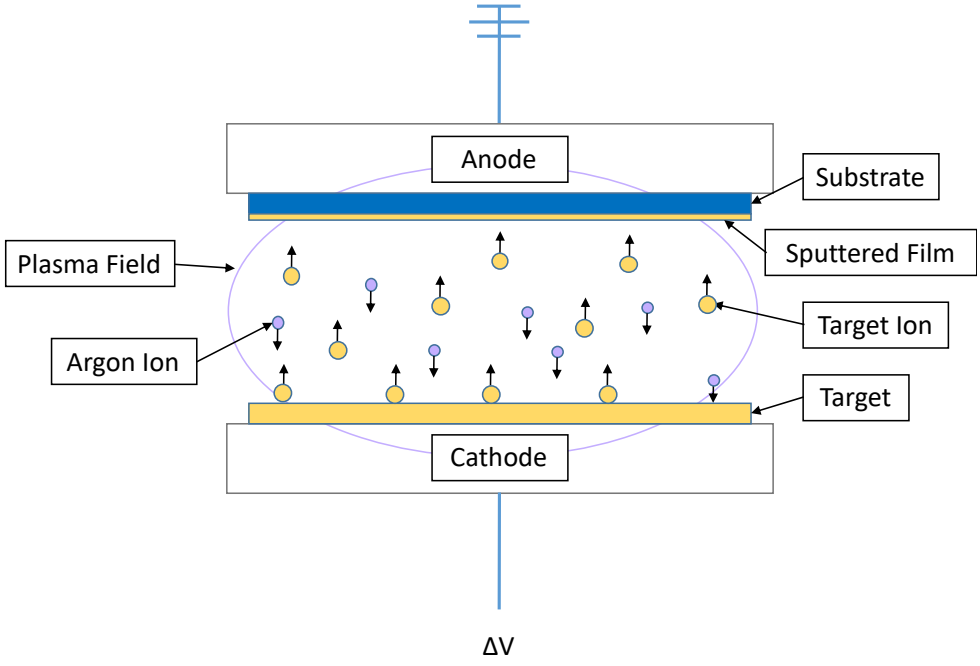

Figure 2.2 Deposition by Sputtering

The substrate can be a variety of materials but is most commonly glass, ceramic, or a crystalline structure like silicon dioxide on the surface of a silicon wafer. As particles are deposited onto the substrate, a thin film develops. The deposition quality is dependent on the energy of the ions from the target material and is controlled by the concentration of reactive gas, the pressure of the surrounding gas mixture, the temperature of the system, and the distance of the target to the substrate [4]. Any surface treatment on the substrate can also impact the deposition quality [3].

This method would provide precise deposition of particles to a desired thickness. However, this application is designed for nanoscale layers of material deposition, with deposition rates varying from 4 nm/min to 25 nm/min [3]. This makes sputtering even slower than evaporation; additionally, sputtering is less able to maintain the chemical composition of the evaporated material and produces a less conformal layer of deposition than evaporation [1]. Thus, this methodology provides a deposition rate too low for the size scale investigated in this study.

2.1.4 Traditional End Milling

Another material removal machining technique is standard end milling. End milling is a machining process that removes material of a substrate by cutting through it with a rotating cutting bit. Specialty bits are made to cutter diameters as small as 25.4 μm with a maximum depth to diameter ratio of 3:1 [5]. This tooling method is typically applied to micro-fluidic channels or components and sometimes jewelry. The bits are made from materials that have very high Rockwell Hardness ratings, typically at least 40-52 HRC, making them very brittle. Due to the nature of their size, it is difficult for machinists to detect issues as the end mill operates, making these bits very susceptible to breaking. The life of a single bit can be as low as 5 minutes under typical operating circumstances [5]. Several factors impact life such as bit size, cutting time, substrate material, and substrate surface finish. The best materials to cut with a micro end mill are softer materials such as aluminum, copper, brass, titanium, and polymers. The grain structure of the substrate is also a critical factor as any random hard spots in the material could cause the bit to break. Reducing the cutting rate will also help in lengthening the life of the bit [5]. Figure 2.3 shows some examples of micro-scale end mill bits.

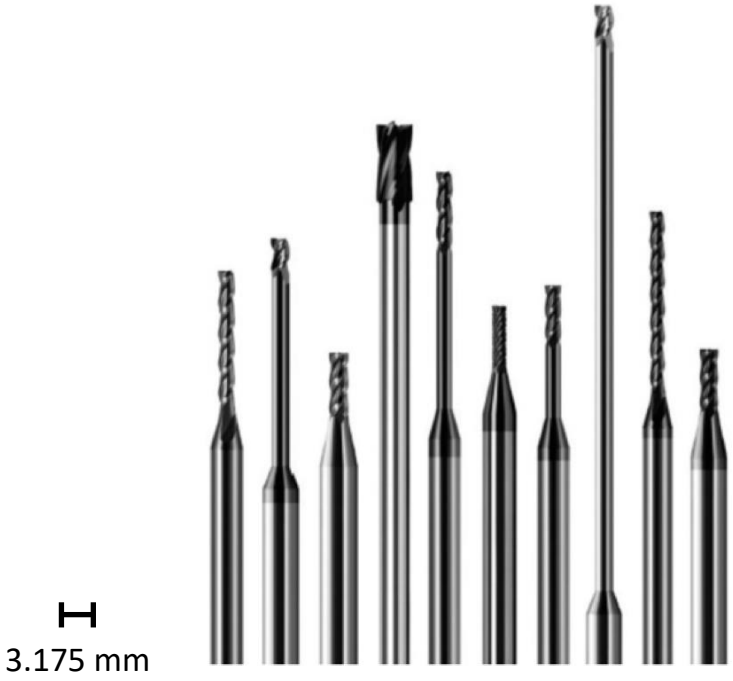

Figure 2.3 Examples of Micro-Scale End-Mill Bits [5]

Micro End-Milling is a viable microfabrication option for features that do not require large amounts of machining, such as singular channels in a polymer plate. However, for multiple samples of long channels, the amount of materials it would require would not be cost or time efficient.

2.1.3 Wire EDM

Wire Electrical Discharge Machining (EDM) is a form of machining that uses electro-thermal erosion to remove material from an electrically conductive material [6]. While it is typically applied to metals, certain specialized Wire EDM applications can cut glass and other electrically conductive materials [7]. The Wire EDM functions by continuously spooling a line of electrically charged wire very close to the surface of the substrate being machined. The current travels from the wire to the substrate, eroding material away when the spark from the interaction heats the substrate to melt. The melted particles are washed away continuously with a stream of deionized water. The shape or pattern created by the EDM is controlled by a CDC or a programmable x-y stage that the substrate is clamped to [7]. Because the wire does not contact the surface of the substrate, Wire EDM offers a machining process that prevents surface imperfections like burrs from occurring, creating a more controlled surface finish [7]. Figure 2.4 illustrates this configuration.

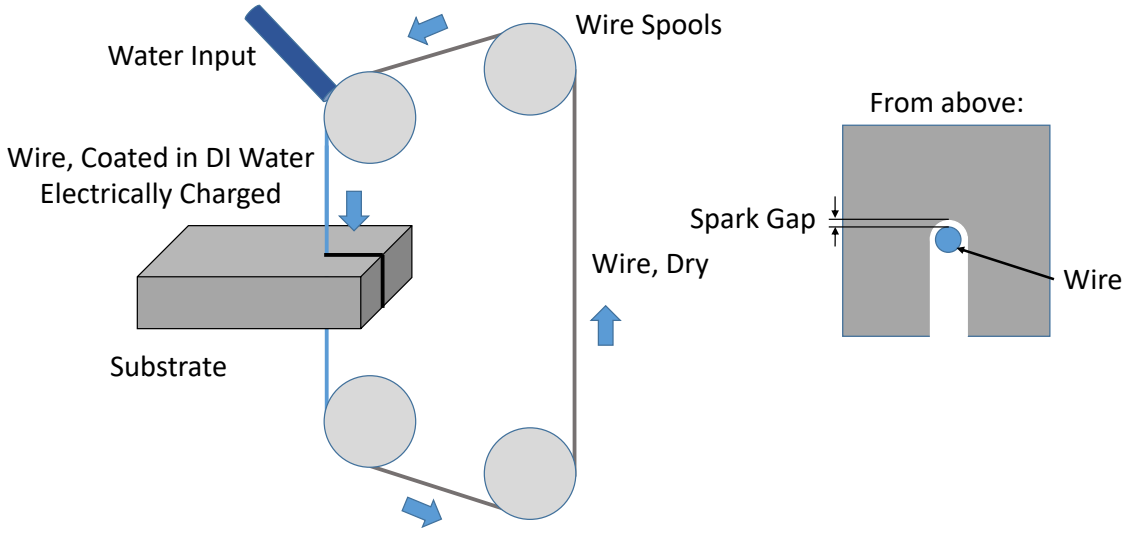

Figure 2.4 Wire EDM Process

Minimum feature size and resolution is controlled by the diameter of the wire, the vibration of the wire as it is spooled, and the amount of discharge energy created by the current exchange [6]. The minimum feature size can be expressed as shown in (2.1 where l_{min} is the width of the resulting cut, D_{wire} is the diameter of the wire, and Gap_{spark} is the spark gap or the distance away from the wire where material is removed due to the electric charge.

$$l_{min} = D_{wire} + 2(Gap_{Spark}) \qquad (2.1)$$

The diameter of the wire can be as small as is available (as small as 5 μm). However, the vibration of the wire as it spools will cause imperfections or notches in features if the wire is not taut enough. With wires of very small diameter (<20 μm), the tension in the wire becomes difficult to control without inducing breakage [7]. In addition, the spark gap distance can be controlled by reducing the discharge energy to a minimum spark distance without losing enough current to still create as spark is 1μm [7].

Wire EDM is a tooling method that allows for a wide variety of feature sizes and geometries that can be made from many materials. Where Wire EDM is a very viable option to make a single sample or small batch of samples of high-aspect ratio patterned features, the time and equipment costs of this method are not ideal for large scale fabrication.

2.2 Motivation

With the availability of many microscale manufacturing methods, it is possible to develop a variety of feature types. However, the additive processes (evaporation, sputtering) are too slow to generate tall features, and the subtractive processes (wire EDM, traditional machining) are expensive and slow for generating a large number of features. Additionally, these microscale manufacturing techniques are well defined and established for generating high fidelity features with heights at most around 150 μm. On the other hand, standard (i.e., not "micro") machining techniques can be used to fabricate features as small as 500 μm. Thus, there is a need for a cost efficient method to create patterned metallic microscale features with high aspect ratio and heights between 200-500 μm tall.

While the technique described in this thesis was developed with a highly specific geometry and application in mind, it can be used for many technologies like electronics, microfluidics, and possibly even artistic applications. The methodology proposed offers a lower cost per part and ability to develop desired features in house without the need for prior machining knowledge or expensive equipment, expediting the replication of the pattern. This study investigates modifying traditional microscale techniques and employing electroless nickel plating to create patterned metallic features between the microscale and standard scale quickly and inexpensively.

2.2.1 Project Overview

This thesis describes work done to develop a novel microfabrication technique that uses electroless nickel plating to generate high-aspect ratio microscale features. This method is detailed in Figure 2.5 in which (a) first, a patterned mold with high aspect ratio features is created using photolithography (as described in Chapter 3). (b) The mold is then inverted and brought to contact with the surface of the metallic substrate and (c) the system is submerged in a plating solution and allowed to plate to a desired height. (d) Once plating is complete, system is removed from solution and the mold is removed from the substrate surface where (e) the remaining metallic substrate results in the inverse of the mold

pattern. This goal of this method was to provide a less expensive, more accessible, and easily repeatable alternative to the techniques listed in Section 2.1.

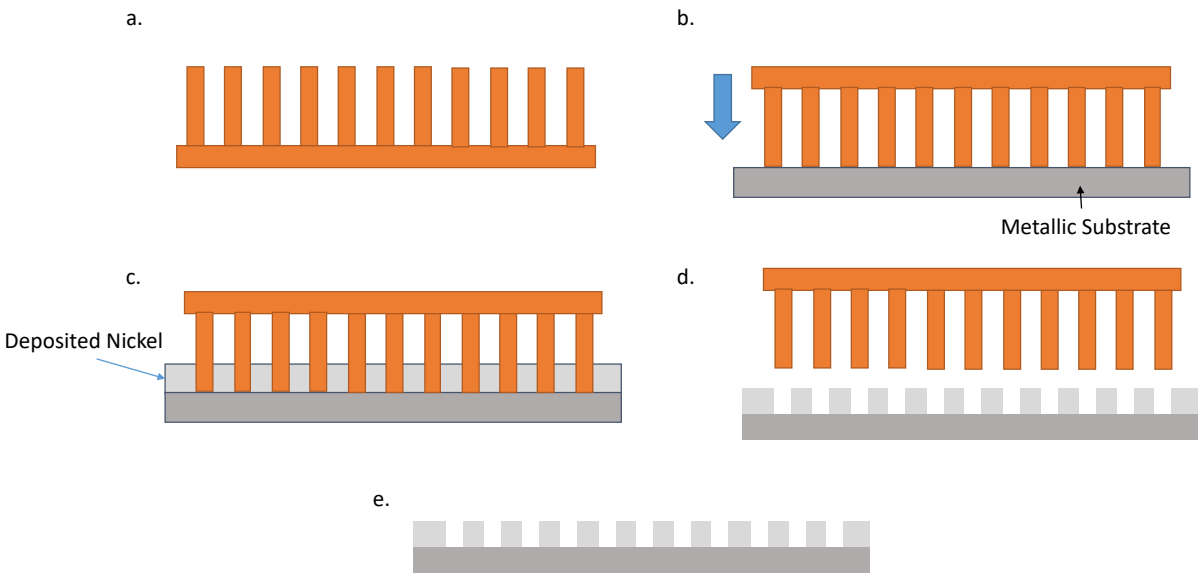

Figure 2.5 General methodology of patterned metal microfabrication

Chapter 3 High Aspect Ratio SU-8 Features

The overall goal of this project was to create patterns of tall metal features with relatively thin width (i.e.,high-aspect ratio features) for use in polymer injection molding applications. The target height of the metal plated features was 250 μm with a feature width of 70 μm, which is a height to width ratio of about 4:1. This chapter details the development of the polymer molds created for the ENP fabrication process outlined in further detail in Chapter 5.

In order to achieve mold features with heights above typical microscale manufacturing techniques but smaller than classical machining practices, a new fabrication protocol needed to be developed. This protocol was adapted from the established microscale fabrication method of photolithography, which was modified to include multiple photoresist deposition steps so that features of the appropriate height could be created. This change required adjustments from traditional single-layer photolithography, such as calibrating parameters like the bake time, exposure energy, and development protocol to account for the additional material, as described in the following sections.

3.1 Patterning SU-8 Photoresist

The molds in this work were created from SU-8 photoresist patterned on a silicon wafer. SU-8 is a widely used negative photoresist developed by MicroChem; it was chosen because is well characterized and has high strength, chemical resistance, and adhesive properties. There are multiple formulas of SU-8, which have varying levels of adhesive strength and different ranges of achievable thickness (as determined by its viscosity). SU-8 3050 was used in this experiment because it is capable of producing high layer thickness (45-100 μm) and has better adhesion than other formulations of SU-8. Because photoresist is a UV sensitive material that changes phase when exposed to UV light, any handling of SU-8 in this study was done in a UV and particulate filtered clean room.

Photolithographic patterning of SU-8 is a multiple-step process. First, a layer of SU-8 is spun onto a silicon wafer by pouring a small amount of the liquid photoresist onto the wafer and placing it in a spin-coater. Inside the spin-coater, the wafer is rotated about its axis at a high velocity for a prescribed amount of time to achieve a uniformly thick layer of SU-8. The thickness of the layer is dependent on the angular velocity and viscosity of the material, which can be found using equation (3.1) below.

$$t = \frac{KC^{\beta}\eta^{\gamma}}{\omega^{\alpha}} \qquad (3.1)$$

In this equation, ω is the angular velocity of the spin coater, η is the viscosity of the SU-8, and the remaining variables are empirically-determined constants. Figure 3.1 illustrates the spin coating process: a.) starting with a clean silicon wafer, b.) SU-8 is poured onto the surface before c.) placing the wafer in a spin coater that distributes the material evenly across the surface.

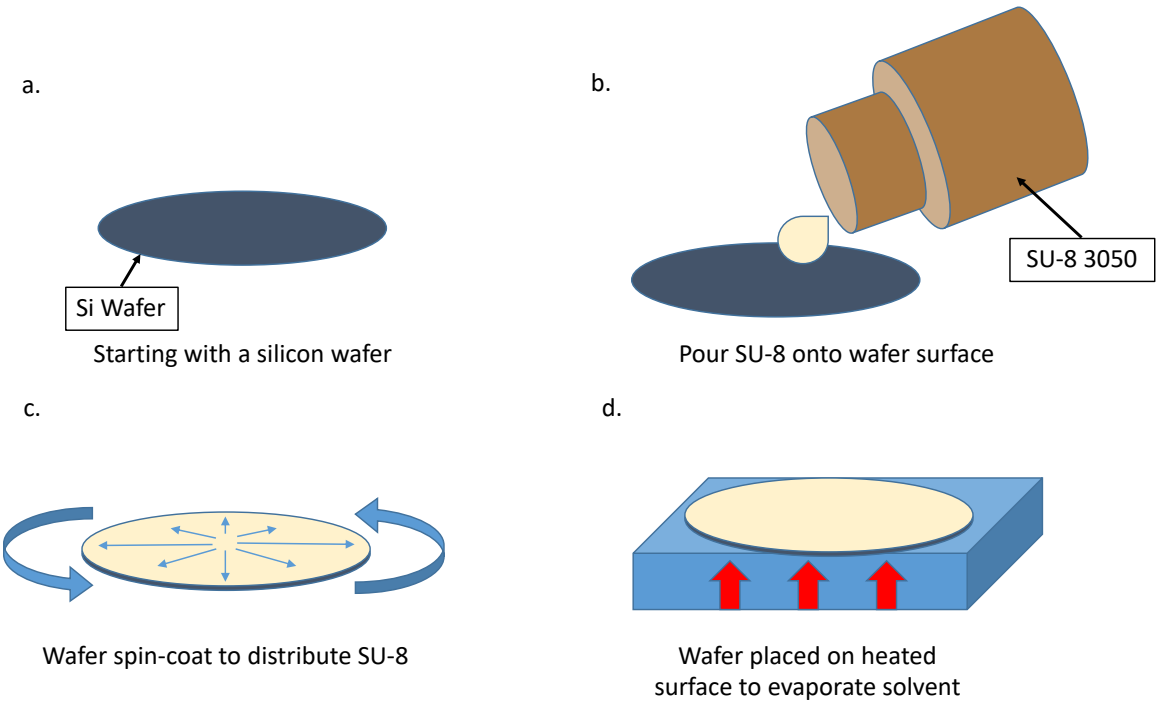

Figure 3.1 SU-8 deposition steps

The thickness of a single layer of SU-8 has been determined by MicroChem for many of their formulations as a function of spin speed, and can be found in published specifications sheet. This is shown in Figure 3.2 for SU-8 3050.

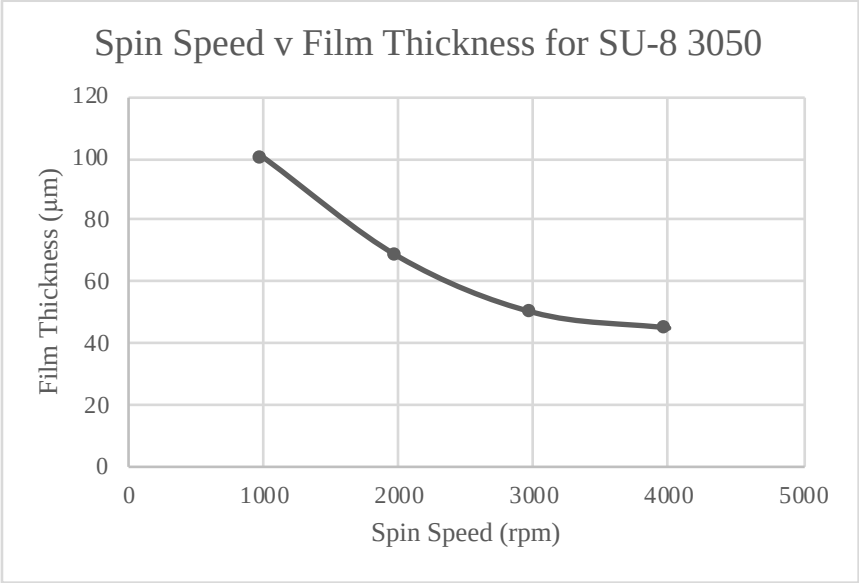

Figure 3.2 Layer thickness of SU-8 3050 series as a function of angular spin speed [8]

Once SU-8 was spun onto the wafer, the wafer was placed either on a hotplate or in an oven, level to the ground, for a designated amount of time and temperature. This procedure is known as prebaking or soft baking, and it is necessary to evaporate a solvent

in the SU-8. Prebaking makes the layer slightly more solid, but in this state, the SU-8 is still soluble. The prebaking times are specified by the technical data sheet from MicroChem for a specific layer height and formulation, as shown in Table 3.1 for SU-8 3050.

Table 3.1 Prebaking time and temperature for SU-8 3000 Series [8]

Thickness (μm)	Soft Bake Time at 95°C (min)
4-10	2-3
8-15	5-10
20-50	10-15
30-80	10-30
40-100	15-45

For each layer spun, this study found that it should be post-baked for the prescribed time with 30 minutes extra for each layer to ensure that enough of the solute would evaporate after leaching, described in section 3.2. After the SU-8 has been prebaked, it is ready to be exposed to UV light. In any area where the SU-8 is exposed to UV light, the exposed SU-8 will cure and eventually become a solid polymer. The UV light is controlled by shining it through a stencil-like tool called a photomask, which is made of a layer of transparent material that has been covered with a layer of opaque material; the opaque layer is etched into a pattern so that the UV light can pass through the transparent material but cannot pass through the remaining area of the opaque layer. Figure 3.3 illustrates this UV exposure step where a.) the photomask is brought to soft contact with the SU-8 and wafer, b.) the photomask and wafer are exposed to collimated UV light, meaning the rays of light are parallel to one another. Looking at the cross section, c.) the UV light passes through any area of transparent material, but does not pass through the opaque material.

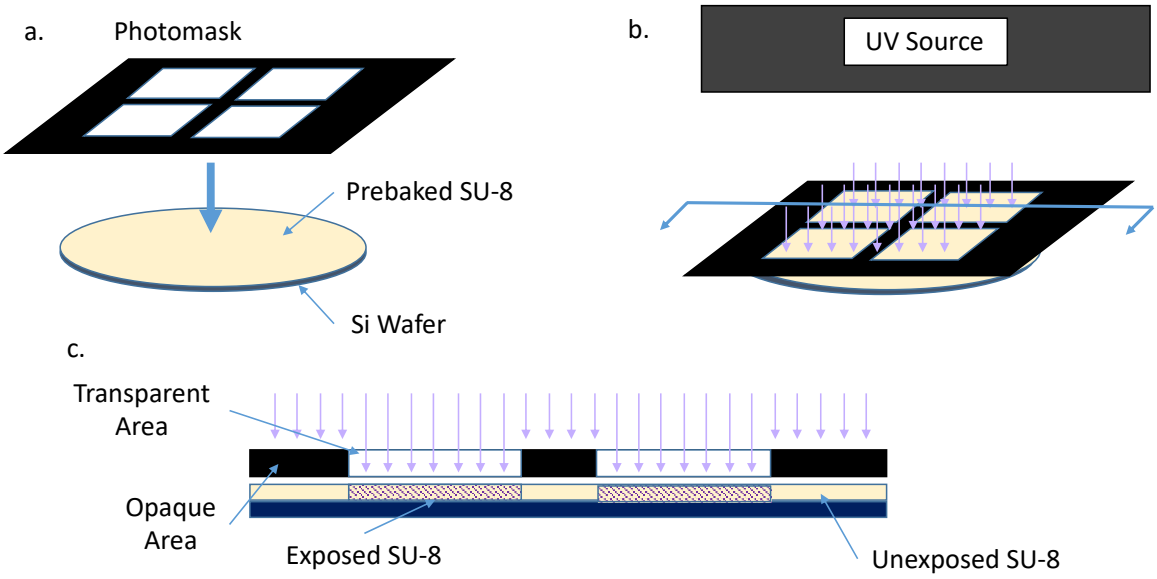

Figure 3.3 UV Photopatterning of SU-8 with a photomask

The alignment and UV exposure step are performed by placing the mask and the wafer into a device called a mask aligner, which brings the mask into very near contact with the SU-8. The mask aligner uses a UV lamp with a lens that creates collimated UV light. This ensures that the features will have close to perfectly vertical side walls. The mask aligner also uses a mechanism that brings the wafer into "soft contact" with the photomask, so that the two components are touching but very little pressure is applied. A gap between the surfaces could cause issues with the exposure due to the beams of UV light no longer being parallel to each other. Distorted UV light would cause distorted features. Figure 3.4 shows a concept of the mask aligner stack up.

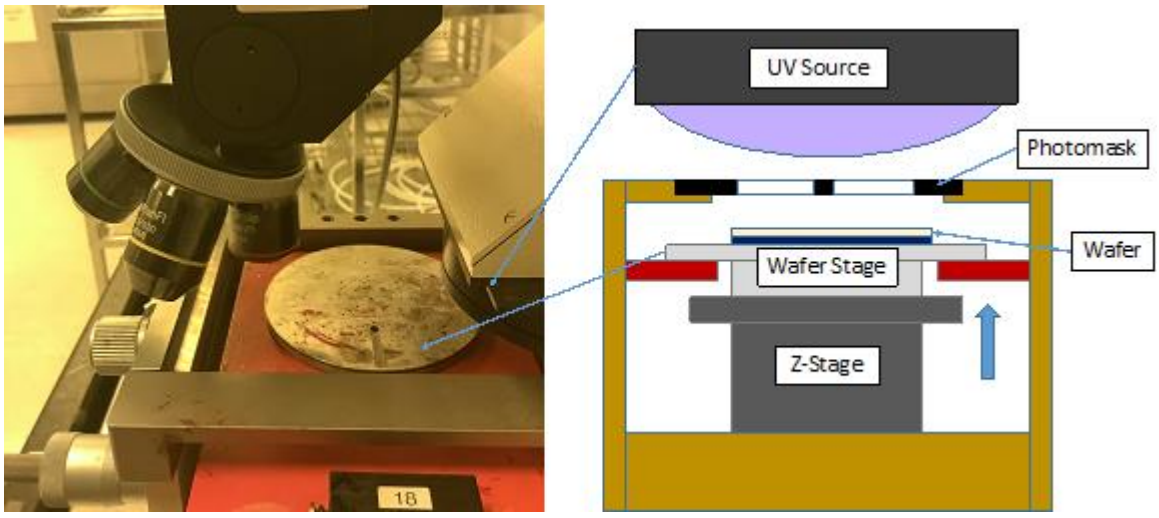

Figure 3.4 Mask aligner to bring wafer to contact with photomask

Once the mask is in soft contact with the SU-8, the apparatus is exposed to UV light for a duration of time determined by the intensity of the bulb and the energy per unit area necessary to cure the specific height of SU-8, as shown in Table 3.2.

Table 3.2 Exposure Energy for SU-8 3000 Series [8]

Thickness (µm)	Exposure Energy (mJ/cm2)
4-10	100-200
8-15	125-200
20-50	150-250
30-80	150-250
40-100	150-250

When SU-8 is exposed to UV light, a photoacid generator called triarylsulfonium hexafluroantimonate salt contained in the SU-8 polymer solution breaks down to produce hexafluoroantimonic acid. The acid reacts with a thermosensitive epoxy called Bisphenol A Novolak epoxy oligomer to create cross-links between the oligomer molecules. This reaction is unique in that it generate in high degree of cross-linking, resulting in optimal mechanical properties such as a high degradation temperature and a modulus of elasticity of about 5 GPa [9]. Figure 3.5 shows a contrast of unexposed SU-8 and exposed SU-8 with cross-linked polymers where a.) details the hexafluoroantimonic acid production when the SU-8 is exposed to UV light, b.) illustrates how the presence of the acid initiates the polymer cross-linking when exposed to heat, and c.) shows the final result after development where the cured SU-8 remains.

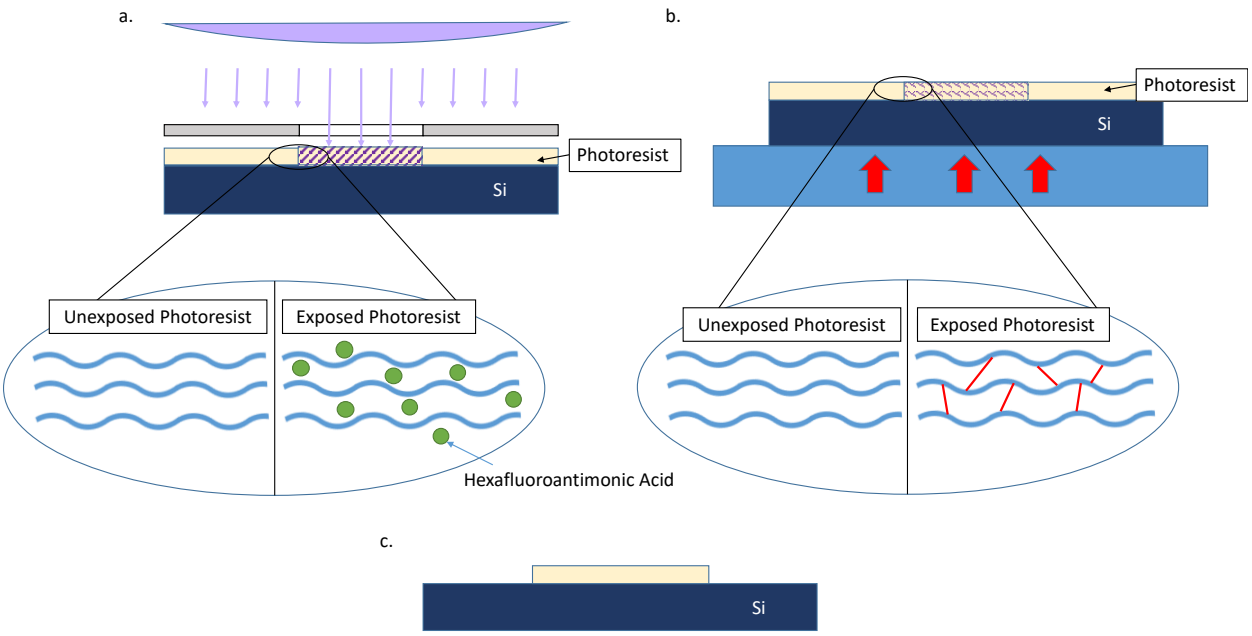

Figure 3.5 SU-8 UV exposure material cross-linking

After exposure, the contact is released and the wafer is moved to a hotplate or oven for another bake session, known as post-baking. This step speeds up the polymer cross-linking in areas of the SU-8 that were exposed to UV light. The duration of the post bake is determined by the height and formula of SU-8, indicated by the formula specifications provided by MicroChem, shown in Table 3.3.

Table 3.3 Post-Baking Specifications for SU-8 3000 Series [8]

Thickness (μm)	Post Bake Time at 65°C (min)	Post Bake Time at 95°C (min)
4-10	1	1-2
8-15	1	2-4
20-50	1	3-5
30-80	1	3-5
40-100	1	3-5

Because the height of the SU-8 in the samples of this study exceed the published step, the ramp up and post-bake times are scaled by the ratio of the expected height to the maximum published height. After post-baking, any uncured SU-8 is dissolved in a chemical bath, also produced by MicroChem, formulated specifically for SU-8 to dissolve any non-cross-linked polymer. Once only the cured SU-8 features remain on the surface of the wafer, the developer is rinsed away with isopropyl alcohol (IPA).

3.2 Spinning multiple layers for taller features

To achieve the required feature height, multiple layer spin steps were performed based on the scale of the SU-8 3050 at the lowest spin speed (1000 rpm), per the SU-8 3000 specification, resulting in an average layer height of about 120 μm. This value was measured after deposition and slightly exceeds the expected spin height of SU-8 3050 from Figure 3.2. This deviation is likely due to the conditions in the cleanroom used to create the sample not matching the conditions of the SU-8 MicroChem used to write the standard, such as lower ambient temperature. Each spin step was performed with the same volume of SU-8 deposited at the same spin time and speed so that each layer would have equal height. The initial spin step was performed on a clean 3-inch wafer using about 3 mL of SU-8 3050; because this formulation of SU-8 is a highly viscous fluid, it was poured slowly in the center of the wafer to avoid introducing bubbles into the SU-8 layer. The wafer and SU-8 were then placed in a vacuum spin coater and spun at a rotational velocity of 1,000 rpm for 30 seconds. Once the SU-8 was spun, it was then placed on a level hotplate for the prebaking step.

After the prebaking step, the wafer was allowed to cool at room temperature on a level surface; at this point the SU-8 polymer was partially solidified due to the evaporation of the solvent. Once the SU-8 was cool, a second layer of SU-8 was spin-coated and then prebaked, using the same volume and spin speed as the first layer. It was important that the wafer was prebaked immediately after spin-coating the second layer, in order to

ensure that the solvent in the unbaked newly deposited SU-8 would not leach and dissolve the already baked SU-8, as shown in Figure 3.6. This would, in effect, partially change the first layer from a solid back to a liquid, affecting the uniformity and integrity of the spin step [10].

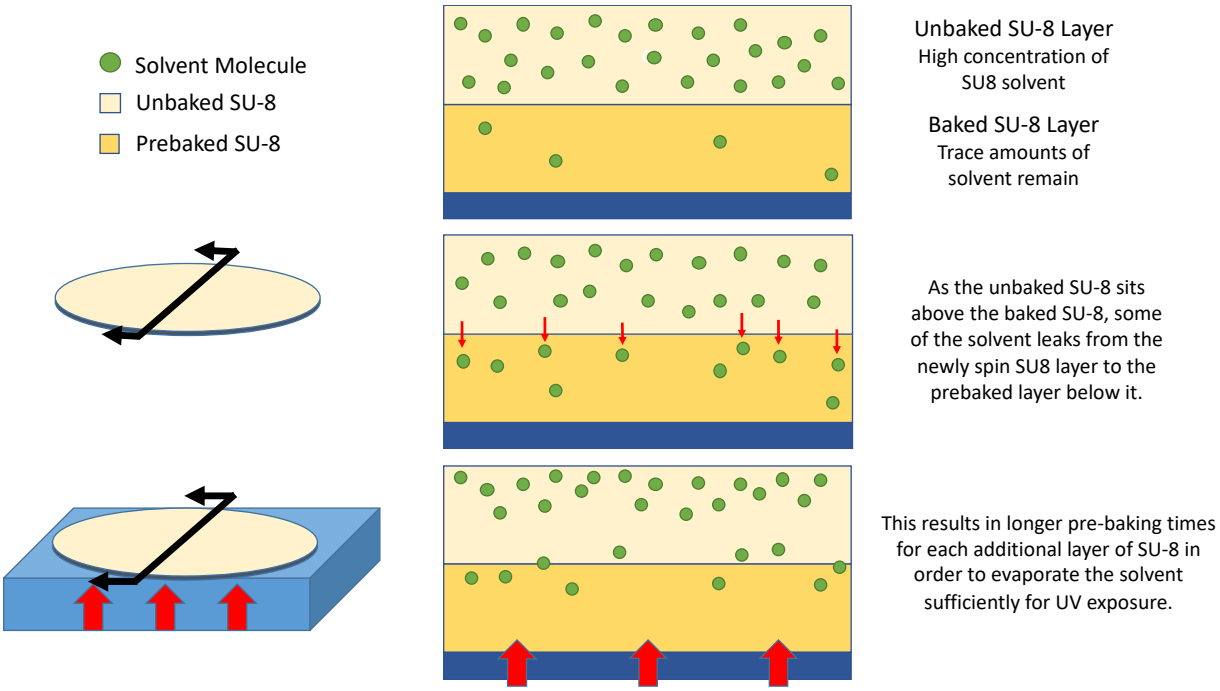

Figure 3.6 SU-8 multiple layer solvent diffusion

In addition, this study found that if enough solvent has not evaporated from the SU-8 layers, the adhesion between the UV exposed SU-8 and the silicon will not be sufficient to withstand the chemical development step. The resulting patterned features will either dissolve or delaminate from the wafer.

3.3 Baking Surface Temperature and Levelness

The levelness of the baking surface and the uniformity of the temperature distribution on the wafer were found to be limiting factors to achieving a level, uniformly thick layer of SU-8 on the wafer. During the pre-exposure baking step, the wafer and SU-8 are heated in an oven or hotplate to evaporate solvent in the SU-8. The uniformity of temperature on the hot plate is critical to ensuring the solvent has evaporated over the entire surface. Prior to the beginning of this step, the SU-8 is still a viscous liquid, and if the wafer is heated at an angle, the SU-8 will pool and will develop an undesirable incline, as shown in Figure 3.7.

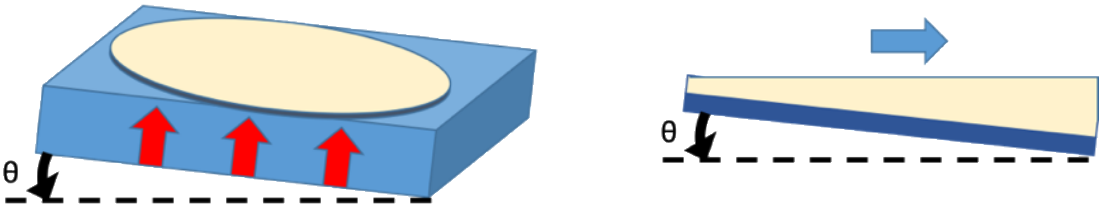

Figure 3.7 Prebaking at an angle

Thus it is important to level the hotplate surface with respect to gravity. In this work, this was done by either using adjustable supports built into the legs of one of the hotplates used or for the other hotplate with fixed supports, layers of paper were used to adjust the angle of the surface. The surface of the hotplate itself was leveled by covering it with a flat layer of aluminum foil. The surface temperature of the hotplate was checked with a thermometer after this covering to ensure that it did not impede the heating of the wafer. After this step, the wafer was allowed to cool on a flat, level surface as well.

3.4 Post-Baking Ramp Up to Alleviate Internal Thermal Stresses

The rate at which the temperature increases and decreases during post-baking affects the internal stresses in the cured SU-8. If the temperature increases or decreases too rapidly, the SU-8 features would visually distort during the crosslinking step while on the hotplate, resulting in the deformation shown in Figure 3.8.

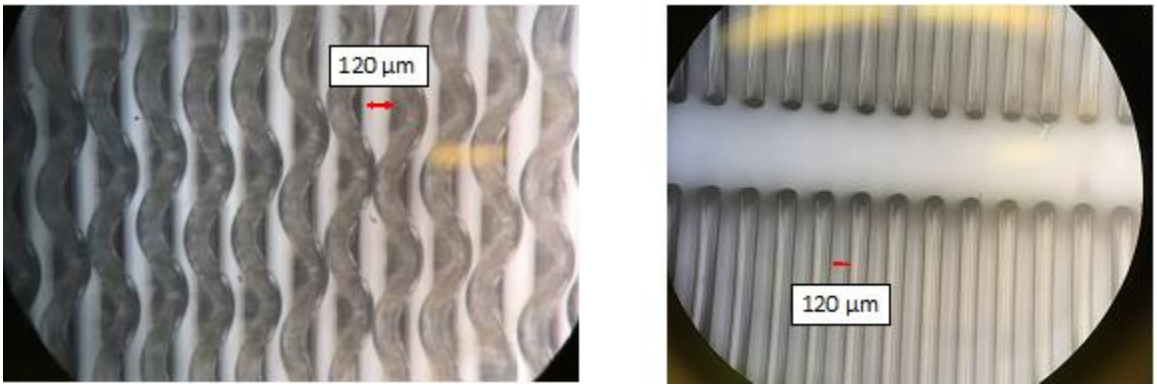

Figure 3.8 Features created using rapid temperature change during post-bake procedure (left) and gradual temperature changes (right).

To solve this issue, the temperature on the hotplate was increased and decreased in increments of 10 °C from 65 °C to 95 °C every 5 minutes which eliminated these effects.

3.5 Surface Adhesion and Capillary Forces

The high aspect ratio SU-8 features were spaced 120 µm apart; during the development and IPA washing steps, these small features were subjected to agitation and capillary forces during drying. In practice, the adhesion between SU-8 and the silicon wafer was not sufficient to support the structures against these force, causing the features to collapse as shown in Figure 3.9.

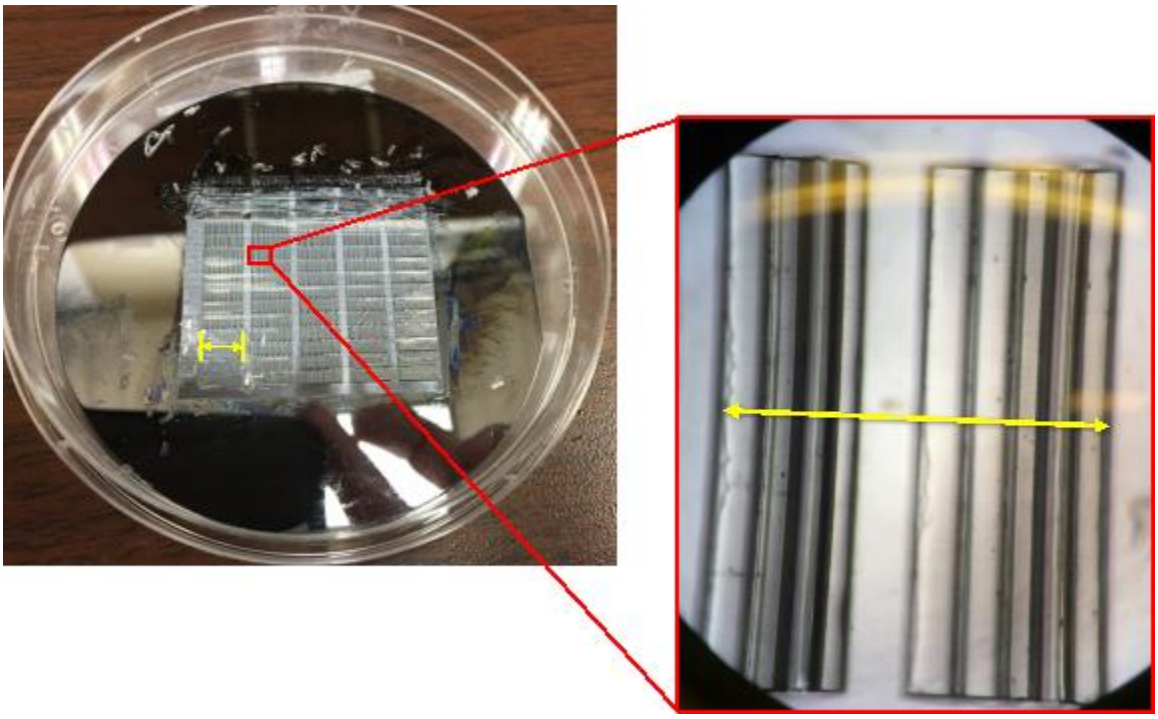

Figure 3.9 Collapse due to insufficient adhesive force during SU-8 development. Scale bars = 6.39 mm (left) and 1.85 mm (right)

Since the adhesion between SU-8 and SU-8 is stronger than the adhesion between SU-8 and the silicon wafer, the adhesion problem was remedied by adding an additional SU-8 layer at the beginning of fabrication. An initial 50 μm thick layer of SU-8 3050 was spun, baked, and uniformly exposed in order to create a solid SU-8 foundation layer on which the high-aspect-ratio SU-8 features were patterned (Figure 3.10). This created a structural base layer that was strong enough to combat the capillary effects of the development and IPA rinse (Figure 3.11).

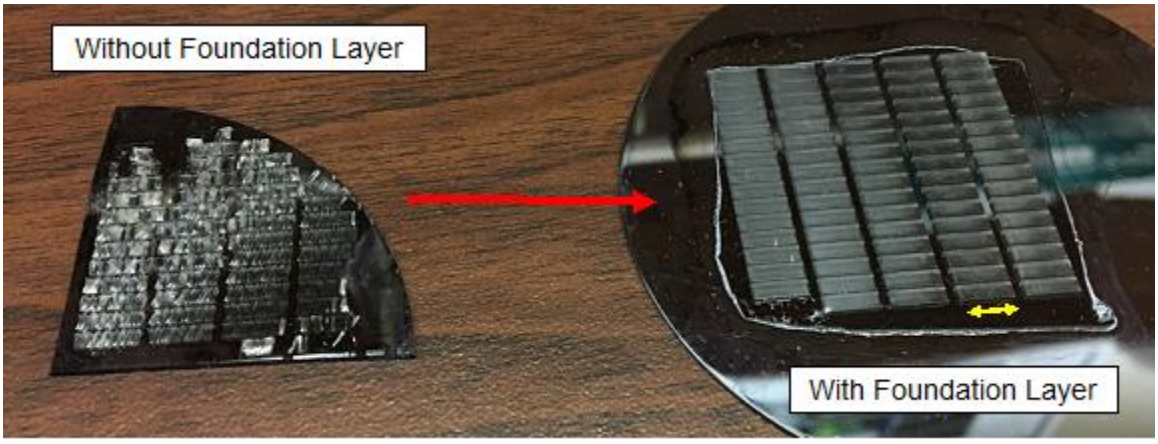

Figure 3.10 High aspect ratio SU-8 features without and with a foundation layer. Scale bar = 6.39 mm

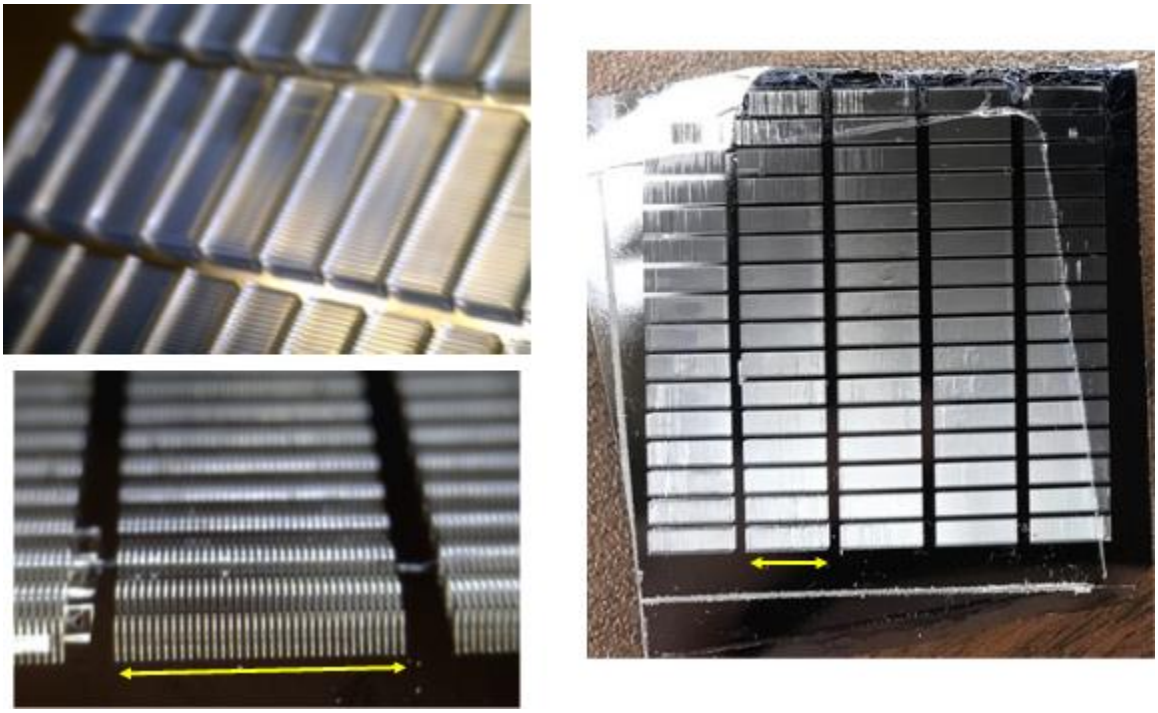

Figure 3.11 Arrays of SU-8 high aspect ratio features.
Scale bars = 6.39 mm

Chapter 4 SU-8 Features with Tapered Sidewalls

This chapter outlines an investigation into the use of inclined lithography to fabricate a pattern of features with angled sidewalls rather than vertical sidewalls. This method, which is a modification of the classic photolithography process presented in Section 3.1, can be used to create features that have an isosceles trapezoid cross-section, as shown in Figure 4.1. This type of geometry could be advantageous for creating SU-8 mold features with a "draft" angle, making them easier to separate from the ENP geometry after plating.

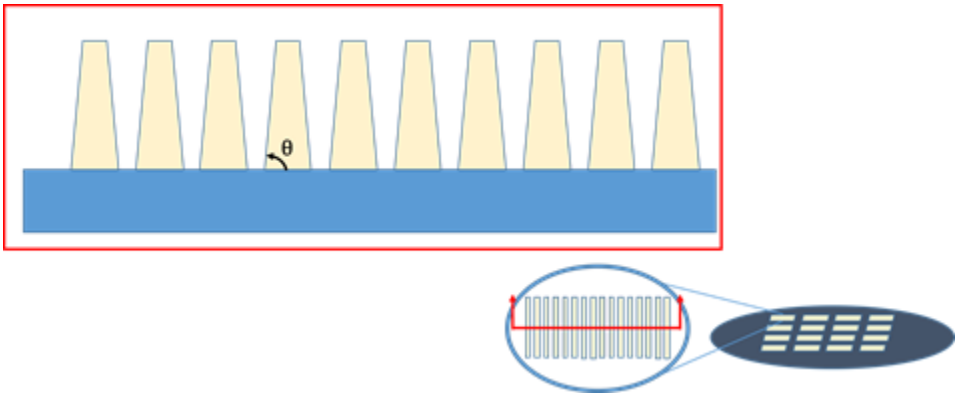

Figure 4.1 Inclined lithography cross section

This methodology was developed and adapted from inclined lithography methods developed in 1994 with the publication of C. Beuret, et al. "Microfabrication of 3D Multidirectional Inclined Structures by UV Lithography and Electroplating." [11]. In the Beuret work, an inclined rotating chuck was used to expose a selectively masked substrate and photoresist, shown in Figure 4.2 to create 10° inclined structures with parallel sidewalls up to 120 μm in height. The Beuret experiment utilized integrated shifted masks to allow for different tilt angles on the same substrate. Figure 4.2 shows the experiment at two exposure angles at different times during the rotation of the chuck. The integrated masks are made using evaporated patterned titanium on the surface of baked negative photoresist. Once the photoresist has been exposed and post-processed, the aluminum sacrificial seed layer and separation layer are removed, leaving just the inclined structure.

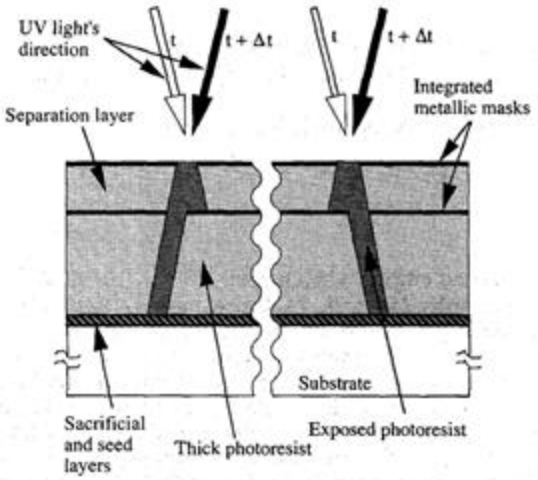

Fig. 1. On this schematic drawing, the inclined rotating exposure of the photoresist through two integrated metallic masks is presented. At time t, only the right structure is exposed, while at time t+Δt, corresponding to a 180° chuck rotation, only the left structure is exposed.

Figure 4.2 Beuret et al. [11] inclined lithography experiment, Copyright © 1994, IEEE

This experiment resulted in angled cylindrical features, as shown in Figure 4.3 .

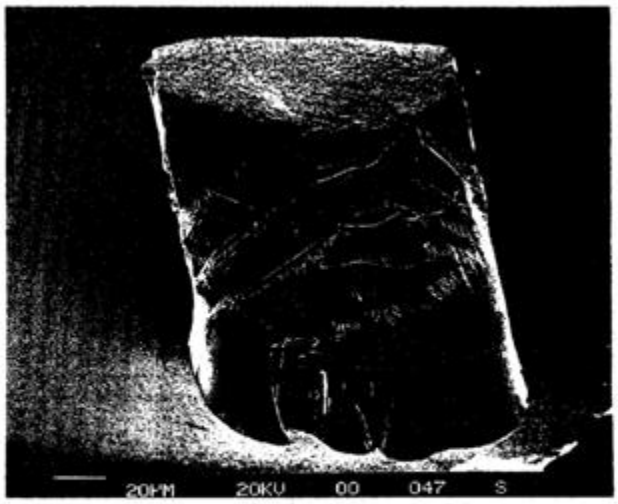

Fig. 4. SEM picture of a 10° inclined 120 μm high structure with nearly parallel sidewalls. On the surface of the structure, some metallic masks residues can be seen.

Figure 4.3 Results from the Beuret et al. [11] experiment, Copyright © 1994, IEEE

The Beuret experiment was developed to have flexible possible exposure angles and the desired results were to generate standalone structures of inclined parallel sidewalls. This study utilizes several ideas from the Beuret experiment but adapted for taller fixed tapered sidewalls structures to remain adhered to the substrate. To achieve a tapered sidewall, SU-8 was cured at an angle to the parallel beams of the collimated UV light source. In this process, many of the steps were the same as traditional photolithography,

such as the wafer cleaning, SU-8 deposition, prebake, post-bake and development. However, during the UV exposure step, the wafer and photomask were placed in an apparatus constructed such that the collimated UV light entered the mask openings at a specific angle. After one round of exposure, the wafer and photomask were rotated such the UV light would enter the mask openings in the mirror-image of the first exposure. This two-step angled exposure method resulted in geometry similar to that shown in Figure 4.1.

4.1 Controlling the Sidewall Angle

In order to achieve a tapered sidewall, SU-8 photoresist must be exposed at an angle rather than normal to the light source. However, because the UV light will refract as it enters different media—for example, the air, glass of the photomask, and SU-8 photoresist used in this work—the angle of the light entering the SU-8 will differ slightly from the initial angle of the light source, as shown in Figure 4.4.

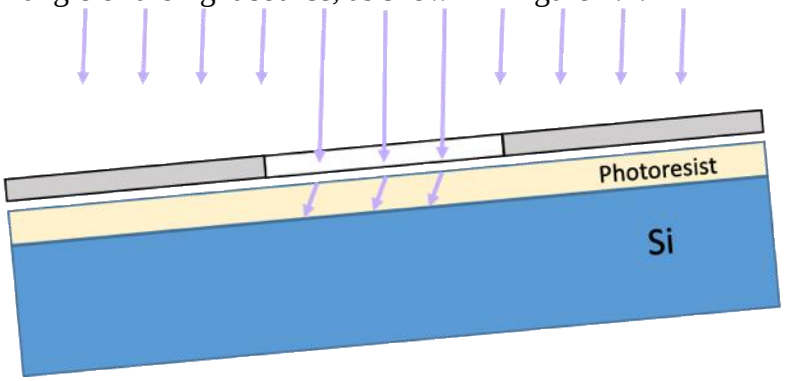

Figure 4.4 SU-8 angled exposure to UV light

To determine the appropriate exposure angle, Snell's Law was applied using refraction indices of the glass of the photomask and the SU-8 resist. At each interface, there is the possibility of light refracting (Figure 4.6). However, because glass and SU-8 have nearly identical refractive indices, the majority of the refraction occurs at the air/glass interface.

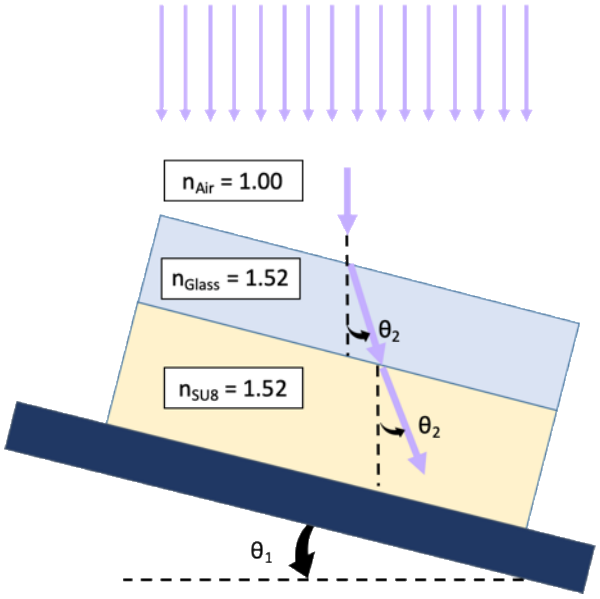

Figure 4.5 Consideration of Snell's Law for angled UV exposure

Applying Snell's law to this problem yields the following relation:

$$n_1 \sin\theta_1 = n_2 \sin\theta_2 \qquad (4.1)$$

where $n_{Air} = 1.00$, $n_{Glass} = 1.52$, $n_{SU-8} = 1.52$, θ_1 is the angle of the tilted stage, and θ_2 is the desired angle of the tapered sidewall.

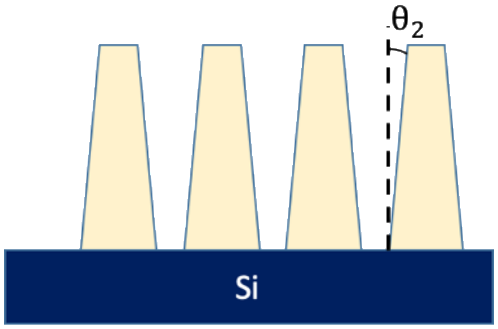

Figure 4.6 Resultant sidewall angle for SU-8 under inclined lithography

For example, the desired taper angle for this experiment was 3°. Therefore, the necessary tilt angle was determined as follows.

$$n_1 \sin\theta_1 = n_2 \sin\theta_2$$

$$\theta_1 = \sin^{-1}\left(\frac{n_2 \sin\theta_2}{n_1}\right) \tag{4.2}$$

$$\theta_1 = \sin^{-1}\left(\frac{1.52 \sin 3°}{1.00}\right)$$

$$\theta_1 = 4.56\,°$$

To achieve the taper on each side of the feature, causing the cross section to be a trapezoid and not a rhombus (one side exposure), the sample was exposed at the same angle on either side of the feature, detailed in Figure 4.7.

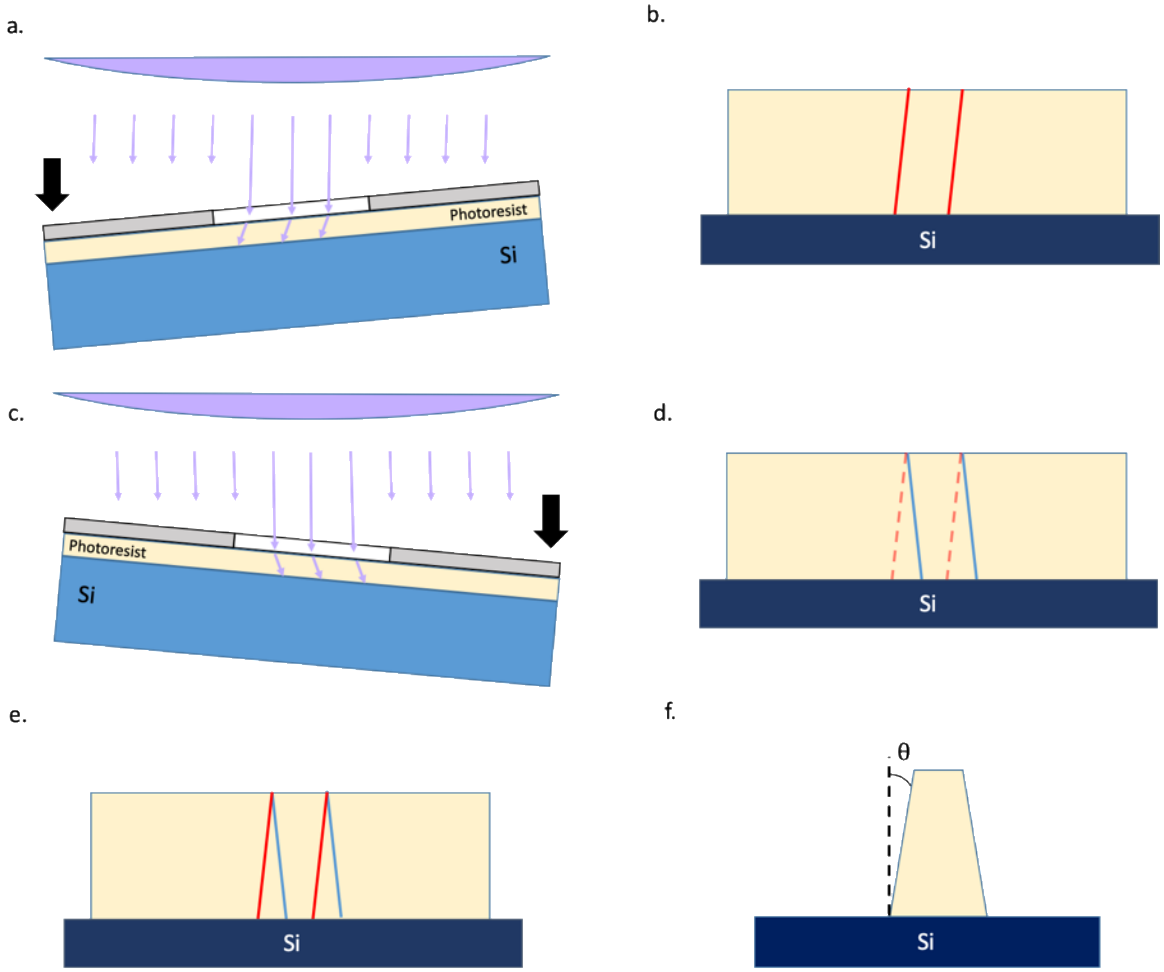

Figure 4.7 Tilted SU-8 exposure steps: a.) SU-8 exposed at positive tilt angle, b.) cross section of exposed SU-8 after exposure, c.) SU-8 exposed at negative tilt angle, d.) blue outline indicates cross section of negative angle, which will include the exposed area of the first exposure step, e.) cross section of SU-8 feature after two step exposure, f.) SU-8 geometry after development

4.2 Controlling the Angle of UV Exposure

To achieve the tilt, an angled platform was designed and 3D printed. This platform, shown in Figure 4.8, was used to tilt the mask and wafer to the angle calculated using Snell's Law in the previous section. The platform was used by first placing the mask and wafer on top of the platform at the platform null position (0°). The mask, wafer, and platform were then placed under the UV source. In order to push the platform to either side of the incline, a small weight is placed on either edge before exposure, rocking the platform over onto one of the flat edges.

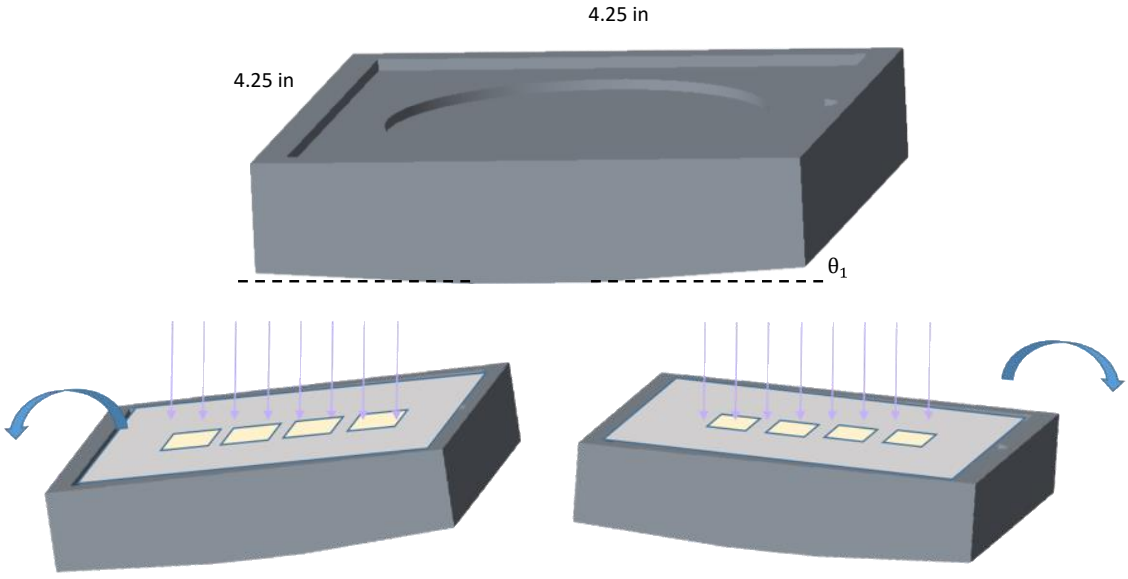

Figure 4.8 Tilting platform for inclined lithography: design of the 3D printed rocking platform (top); once assembled, the platform can be tilted to either side to provide a controlled UV exposure angle (bottom).

The design shown contains features that were originally designed to house the silicon wafer (round indentation in top surface) and mask (rectangular indentation in top surface). However, after several experiments it became apparent that this did not provide adequate control over the contact pressure between the mask and wafer during exposure.

In traditional photolithography, a wafer and photomask are brought to contact using a mask aligner, which has an internal, finely tuned XYZ stage that is carefully calibrated to maintain controlled soft contact. However, the platform shown above did not provide any control over this contact pressure. To remedy this problem, an new contact apparatus was built to be compatible with the tilting stage, as shown in Figure 4.9. In order to bring the wafer to contact with the photomask, the wafer was placed on a Z-Stage; the bottom of the Z-stage was bolted to a metal fixture that held the photomask stationary using a series of retaining plates. By actuating the Z-stage, it was possible to slowly raise the wafer in order to bring it into controlled contact with the photomask. After the wafer and the

photomask were in contact, the entire metal-fixture assembly was placed on the tilting platform. At that point, the assembly was ready for the UV exposure step.

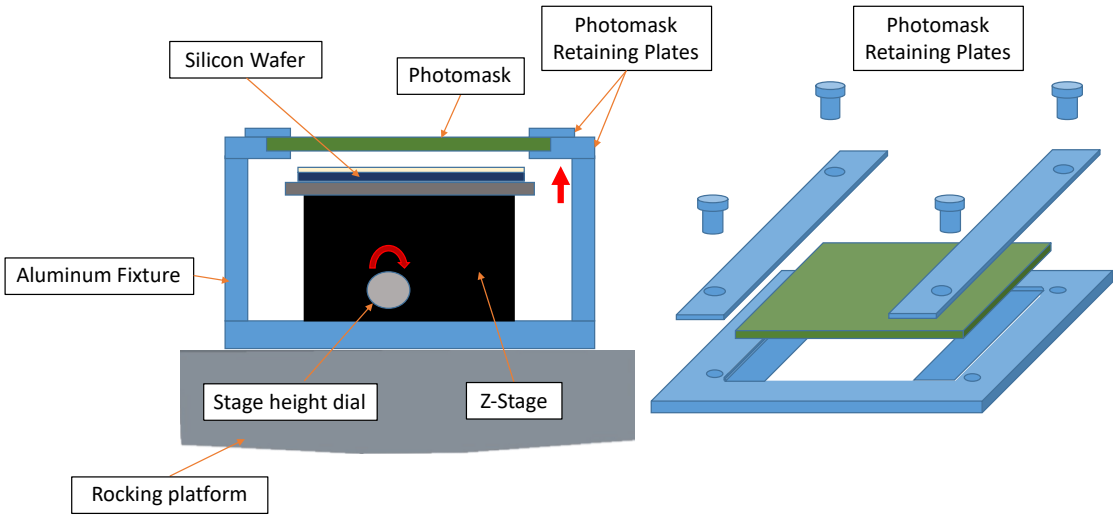

Figure 4.9 Photomask-Wafer contact apparatus

4.3 UV Exposure

The next step in the inclined photolithography process is UV exposure. Because the assembly described in the previous section is too large to fit into a typical mask aligner, another collimated UV source was used, an AB-M LS-63 UV Exposure System (shown in Figure 4.10. This UV source had enough space below the lamp to accommodate the entire photomask-wafer-platform assembly, and it also allowed control over the UV exposure time and energy.

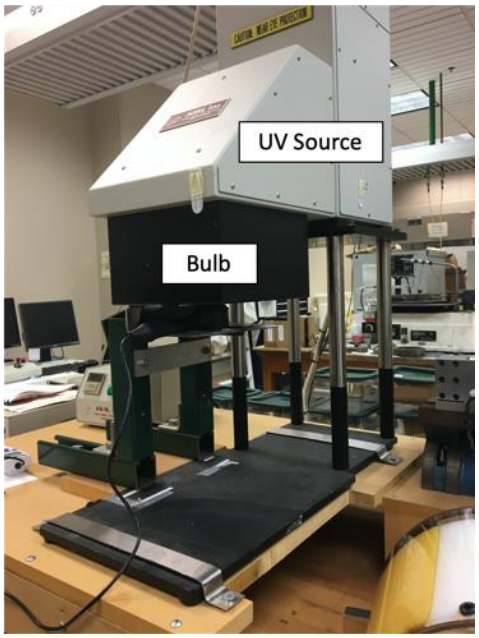

Figure 4.10 AB-M LS-63 UV Exposure System

The collimated UV source used was not located in the cleanroom environment used for spin-coating SU-8 on the wafer, so the sample had to be moved between facilities. Because the SU-8 is photosensitive, it was essential that no light exposure occurred during transport to and from the cleanroom. Aluminum foil was placed over the entire assembly and checked carefully to ensure there were no holes or tears to allow light to reach the wafer. If any were found, the sample was recovered with new foil before leaving the cleanroom. The covered sample was transported to the alternate facility and placed under the UV lamp, as shown in Figure 4.11. A support block was placed under the tilt stage to minimize the distance between the wafer and the UV source. Note that the photomask, Z-stage, and wafer are not included in the photograph.

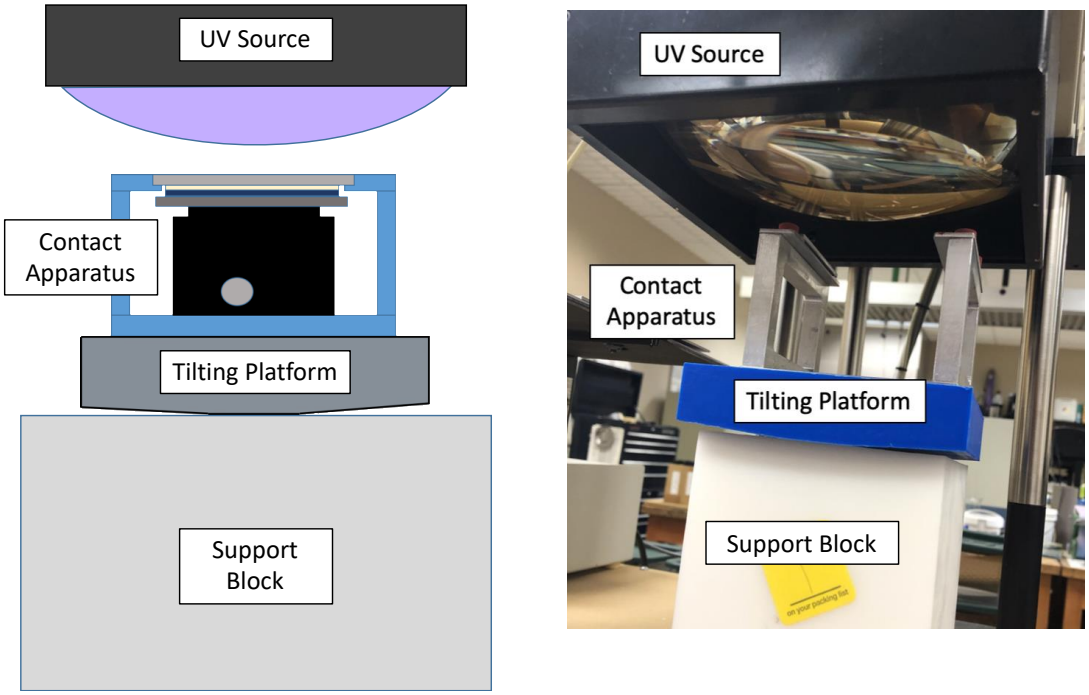

Figure 4.11 Schematic (left) and photograph (right) of the inclined lithography exposure setup

Once the sample was under the lamp, the overhead lights were turned off and a layer of aluminum foil was added around the entire perimeter of the UV lamp bulb cover, in order to minimize ambient light contamination. Only after these precautions were taken was the aluminum foil on the sample removed.

The UV source had programmable exposure time and exposure wattage in mW/cm^2 using the controls shown in Figure 4.12. For the experiments described here, the UV intensity was set to 50 mW/cm^2 and confirmed using a UV intensity meter.

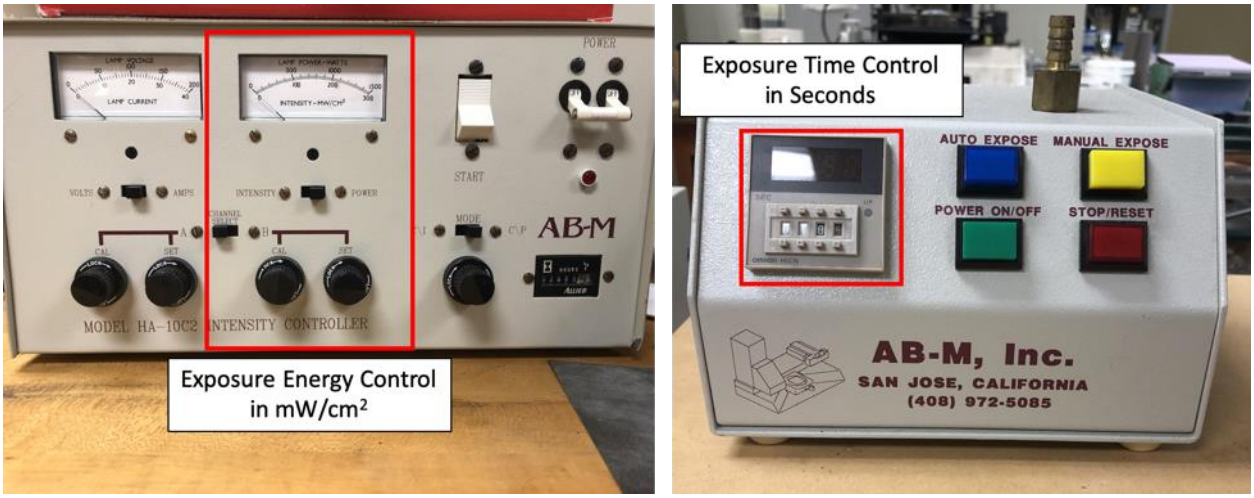

Figure 4.12 UV source control panel

As previously discussed, to get the taper on both sides of the feature, the sample was exposed at the desired angle on either side of the feature. However, this implies that some of the SU-8 was exposed to UV twice, as shown in Figure 4.13.

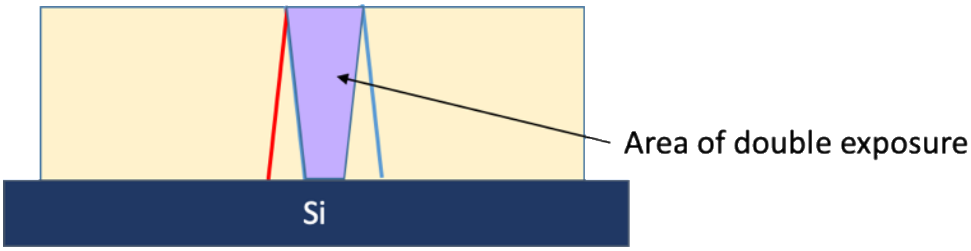

Figure 4.13 Inclined lithography area of double exposure

The crosslinking of the SU-8 polymer is dependent on the amount of energy exposure introduced to the system, in mJ/cm^2. As discussed in Chapter 3.1, the exposure to UV and subsequent postbaking step causes the molecules of the SU-8 to crosslink, solidifying the photoresist in those locally exposed areas. If the resist is underexposed—meaning it does not get enough energy per unit area to crosslink the polymer—the features will have low fidelity and will likely have lower adhesion energy to the silicon wafer surface due to the cross-linking not occurring through the entire layer of SU-8. On the other hand, if the sample is over-exposed—the sample gets more than the necessary energy per unit area—regions outside the exposed areas can also become cured, often resulting in geometry that has an unintended overhang, as shown in Figure 4.14.

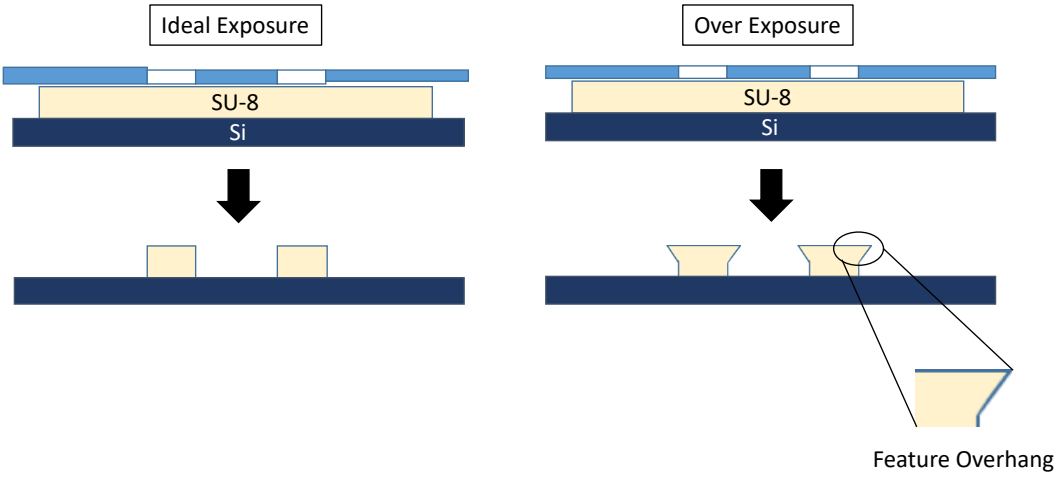

Figure 4.14 Effect of photolithography over-exposure

This phenomenon was documented in del Campo and Greiner [9], as shown in Figure 4.15.

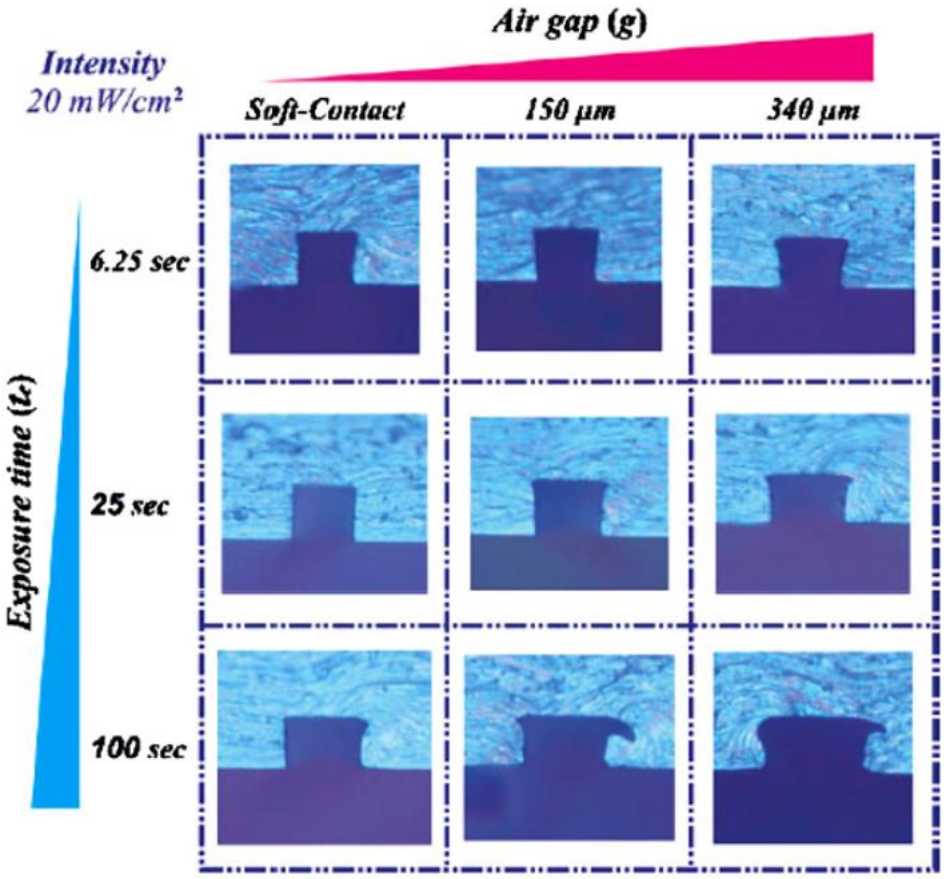

Figure 4.15 Effect of air gap between the photomask and photoresist and excessive exposure energy [9]

In order to provide enough exposure energy to adequately cross-link the single exposure region and avoid causing over exposure issues in the area of double exposure (i.e., minimizing overhang), a series of experiments was performed to determine the optimal single-exposure energy for the system. For 400 μm tall vertical sidewalls, the optimal exposure energy was 350 mJ/cm^2; for features of the same height produced using the tapered-sidewall method, the optimal single exposure energy was found to be 60% of this value. Therefore, each side was exposed to 60% of the recommended exposure energy, while the central overlap region was exposed to 120% of the recommended exposure energy. Note that this value was determined experimentally for this specific set of parameters and may or may not translate directly to other systems. Thus, the applied exposure energy on either side was (0.60)(350 mJ/cm^2) = 210 mJ/cm^2. With an applied UV intensity of 50 mW/cm^2, the exposure time on each side was 4.20 seconds (Figure 4.16).

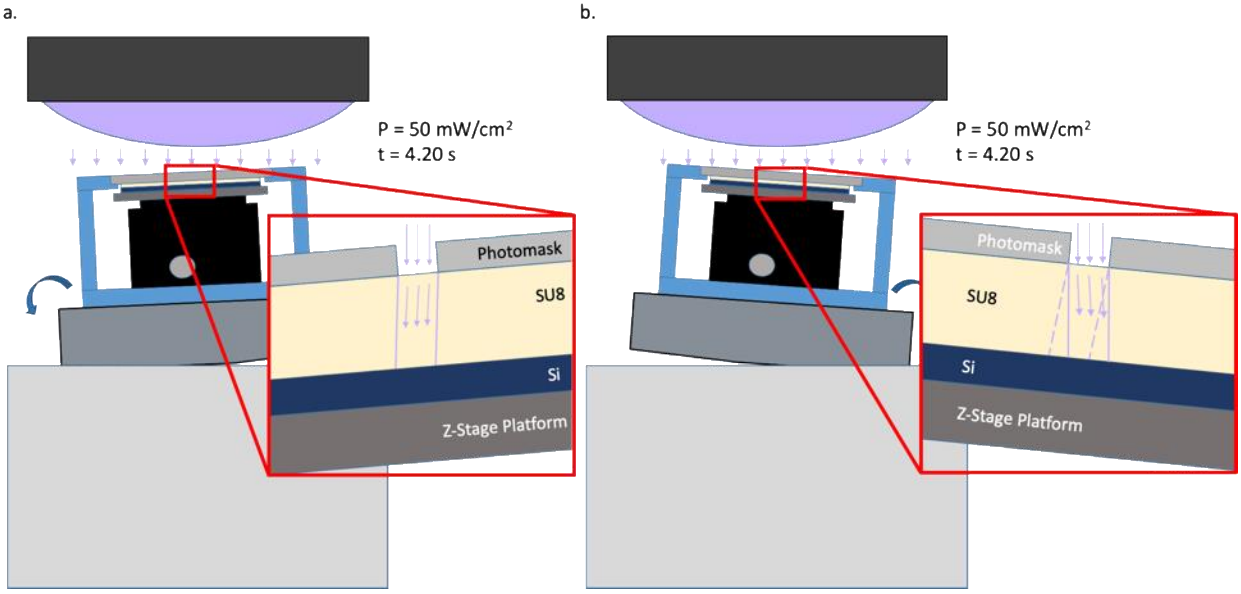

Figure 4.16 Double exposure procedure: sample was exposed to UV light at one angle (a) and then at the mirrored angle (b) to produce trapezoidal features.

Once both UV exposure steps were completed, the UV source was powered down, the sample apparatus was removed from the stand, and recovered with aluminum foil before returning to the cleanroom for post-exposure baking and development. As detailed in High Aspect Ratio SU-8 Features, once the wafer was removed from the contact apparatus, it was post-baked with a slow ramp up to 95°C for 30 minutes and a slow ramp down to room temperature before being submerged in a developer and agitated until the uncured SU-8 totally dissolved. The wafer was then rinsed with ethanol and dried with a stream of nitrogen to ensure removal of liquid between the SU-8 features.

4.4 Inclined Lithography Results

Results from one of the inclined-lithography experiments are shown in Figure 4.17. It can be seen from this image that there are regions of cleanly defined features, but also regions

of feature distortion. In the distorted areas, the SU-8 features separated from the silicon wafer and bunched together during feature post-bake and development. This may have been due to uneven contact pressure in regions of the sample during the UV exposure step.

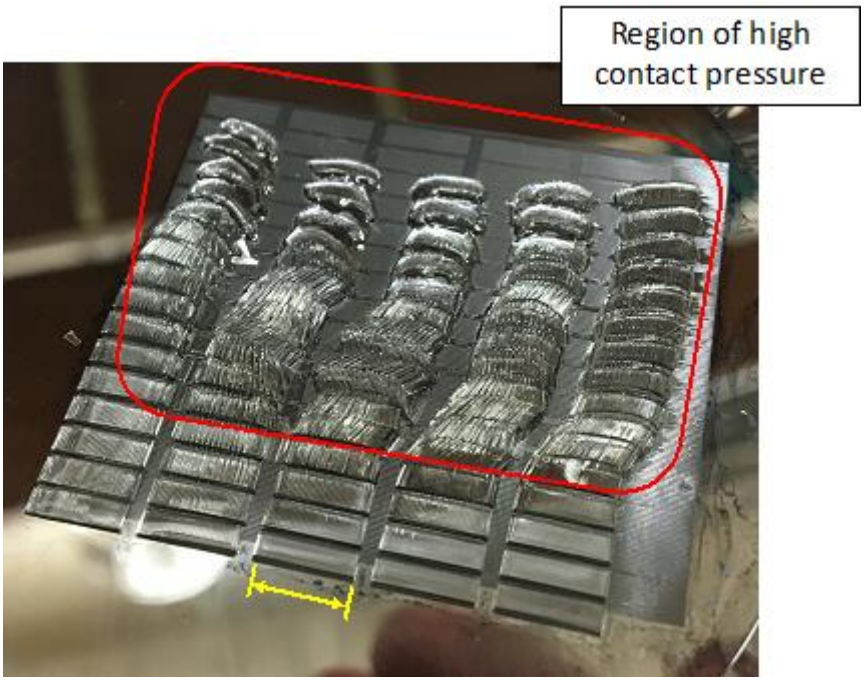

Figure 4.17 Feature distortion during inclined lithography.
Scale bar = 6.39 mm

In order to analyze the geometry in regions that produced in viable features, the SU-8 coated wafer was cast in liquid PDMS (Sylgard 184, Dow Chemical), cured and removed. This PDMS was carefully sectioned using a razor blade and examined under a high-magnification light microscope to yield images such as the one shown in Figure 4.18. These results also show evidence of a slight overhang, which can be expected from a 120% recommended exposure energy that was experienced in these areas.

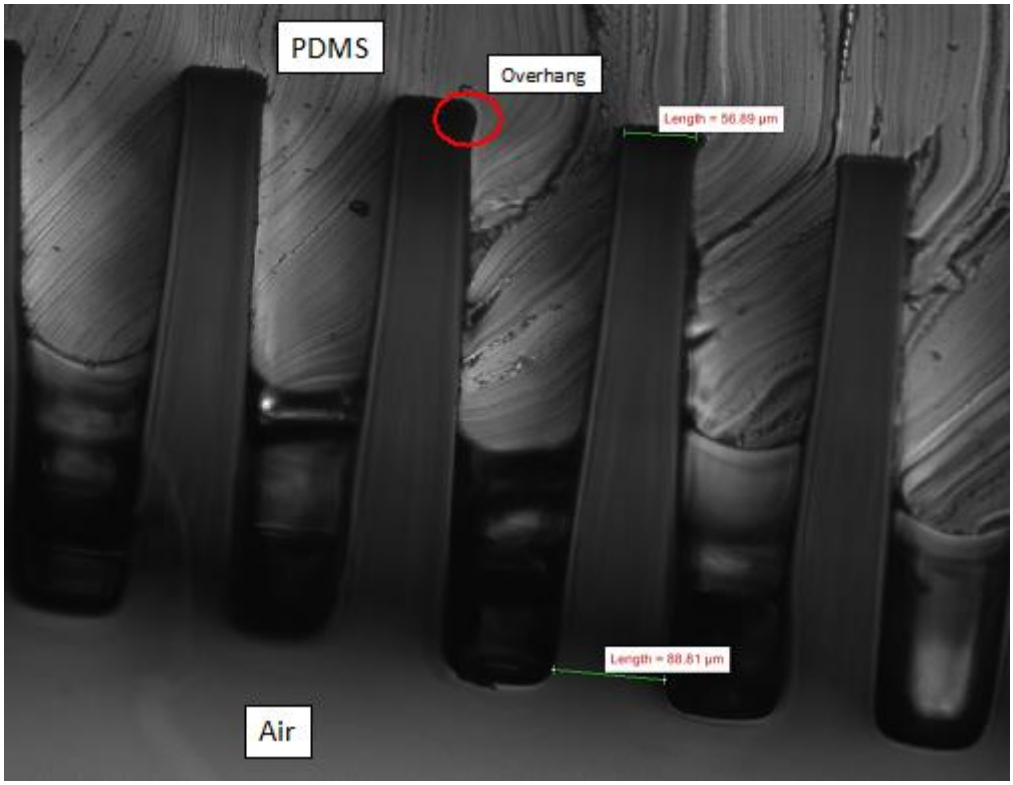

Figure 4.18 Inclined lithography PDMS cast cross section

Using the measurements from the PDMS cross-section, it was possible to calculate the taper achieved in these samples (Figure 4.19). According to these measurements, the actual taper was 3.33°, a very minor overshoot of the desired taper angle of 3°.

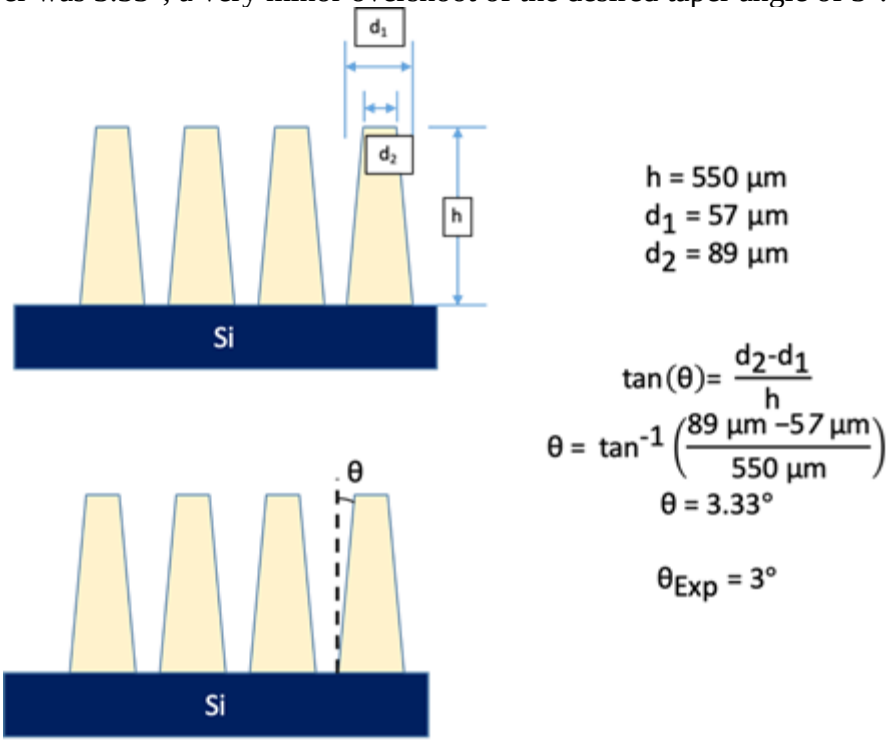

Figure 4.19 Calculations of sidewall taper angle in inclined lithography process

In all, these experiments yielded promising results, albeit only a partial success. In the future, fidelity of the inclined lithography features could be improved with more uniform contact pressure under exposure. The error in the taper angle could potentially be reduced by increasing the resolution of the 3D printed tilt stage or introducing another, more accurate apparatus to introduce an angle to the UV light to the SU-8.

Chapter 5 Micro-patterning using Electroless Nickel Plating SU-8 Patterned Molds

This study investigates the manufacturability of high fidelity metallic patterned features at the microscopic scale. To achieve the desired geometry, a 3D mold was used with a metal deposition method called electroless nickel plating. Plating occurs in the exposed regions of the mold. Therefore, in order to achieve the desired pattern features, the mold was the 3D inverse of the design. In this work, the mold was fabricated using modified photolithography techniques to create a high aspect ratio SU-8 3050 pattern on a silicon wafer. The pattern was plated on a substrate around the mold. An overview of the general process is shown in Figure 5.1 .

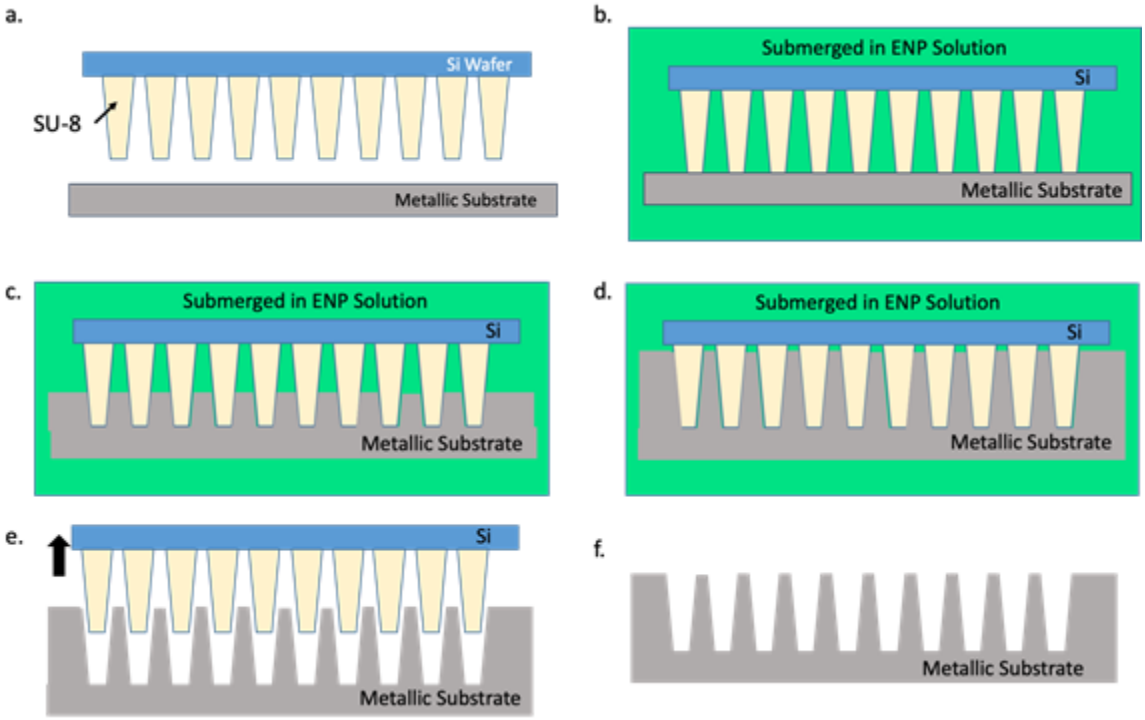

Figure 5.1 Electroless nickel plating using an SU-8+Silicon mold; a.) Mold brought to contact with metallic substrate; b.) mold and substrate submerged in solution; c, d.) ENP process progresses, adding nickel onto the metal surface, forming the negative of the mold; e.) substrate removed from solution and mold separated; f.) final metal geometry results

Electroless nickel plating (ENP) is very similar to electroplating. For electroplating, an electrical current is used to drive a chemical reaction that deposits metal onto an electrically conductive surface. The substrate to be plated is submerged in an electrolytic solution that contains the ions of the desired plating material. When a voltage difference is applied between the substrate and a plate made of the desired plating material, current travels through the solution by removing ions from the surface of the anode and deposited those on the surface of the cathode. ENP is also a method of depositing metal onto a surface due to an ionic reaction. However, ENP is an autocatalytic reaction, utilizing heat rather than current to drive the chemical reaction.

Electroless nickel plating is beneficial to many high precision applications due to its uniform deposition thickness on the surface of the substrate. ENP deposition has a

uniform deposition thickness on entire perimeter of an exposed surface. Whereas, electroplating tends to gather deposition around corners and radii, caused by local variations in current density resulting in the thickness at those locations to be thicker than the open surface of the substrate. This effect can be seen in Modern Electroplating, 3rd Ed. [12], Ch 31. The main factor that contributes to the difference in plating uniformity is that uniformity of deposition in the electrolytic reaction is dependent on the local current density [13]. Current density tends to be higher around sharp corners, which results in higher plating thicknesses.

In contrast, ENP deposition is dependent on contact with the solution, concentration of plating and catalyst ions, and solution temperature. Therefore, during the electroless nickel plating process, nickel should be deposited onto a substrate uniformly and theoretically at a constant rate if all of the previous variables are held constant.

In order to continuously deposit material chemically, ENP utilizes the following oxidation reaction [14]:

$$H_2PO_2^- + H_2O \rightarrow H_2PO_3^- + 2H^+ + 2e^-$$
$$Ni^{2+} + 2e^- \rightarrow Ni$$

The sum of the two reactions results in the following:

$$Ni^{2+} + H_2PO_2^- + H_2O \rightarrow H_2PO_3^- + 2H^+ + Ni$$

Because the hypophosphite (H_2PO_2) acts as the catalyst in this reaction, the deposition rate is dependent on the concentration of hypophosphite in the bath [14].

The ENP solution materials were purchased as a kit from the manufacturer Caswell Plating. The recommendation from the kit manufacturer was to keep the concentration of the nickel source and hypophosphite maintained at a value above 80% of the original concentration. For this study, the hypophosphite salt in the Caswell kit was sodium hypophosphite $NaPO_2H_2$ and the nickel source was nickel (II) sulfate $NiSO_4$.

One limiting property of ENP is that the solution produces gaseous product during the reaction. Due to this byproduct, there must be sufficient space between the mold surface and the plated substrate for gas to escape. As the distance between the mold and the plated material decreases, the bubbles begin to prevent the liquid ENP solution from reaching the substrate surface, in addition to blocking the liquid products of the reaction from diffusing away from the substrate, slowing the reaction. Figure 5.2 shows an example of the bubble formation on an aluminum substrate.

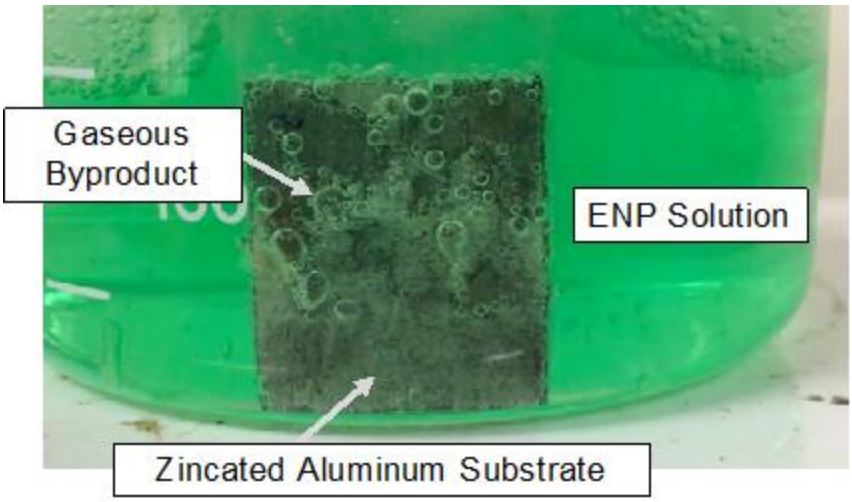

Figure 5.2 Gaseous byproduct during ENP solution

Figure 5.3 shows how the gaseous byproducts may become problematic in the confined space created by the gaps between the metal surface and the SU-8/silicon mold. As the reaction progresses, the gaseous byproduct accumulates at the metal surfaces (Fig a,b). The bubbles grow in size as the reaction progresses, and will eventually dislodge to float away once the size of the bubbles is large enough to generate sufficient force due to buoyancy (Fig. 4c). As the substrate continues to plate, the plating surface gets closer to the mold surface, as shown in Fig. 4d. If there is not enough distance between the mold and the substrate surface, the bubbles can become pinned in place, slowing their escape to the surface. As the removal of the bubbles slows, the diffusion of the ENP solution and other liquid products slows as well, slowing the reaction and therefore the plating rate.

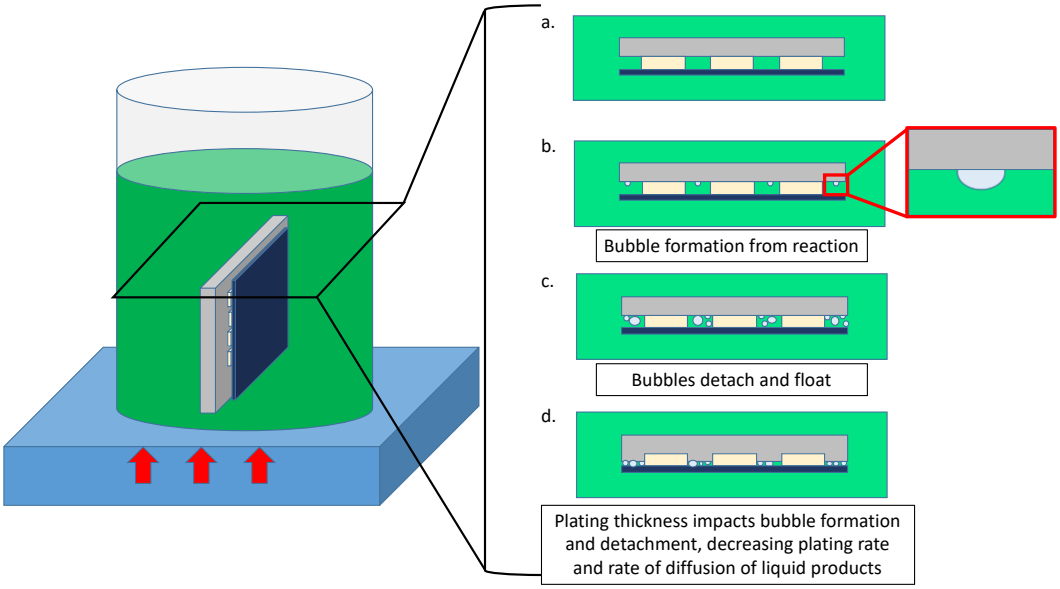

Figure 5.3 ENP bubble formation over time

In order to minimize this effect, the mold-substrate assembly was submerged in the ENP solution such the gaps between the mold and metal were oriented parallel to the direction

of gravity; this helped to take advantage of the buoyancy force on the bubbles when they form. The features on the mold used in this study were also adjusted to include 100 μm of additional height beyond the height of the desired plating level. This allows for the bubbles to escape from the area between the metallic substrate and the mold area and allow the solution to continue to flow and plating to continue.

5.1 Preparing Materials for ENP Process

Multiple plating materials were explored to determine the best option for a plating substrate. The most cost-efficient material for ENP was found to be aluminum. It is compatible with the ENP process, low cost, and easily machined. However, aluminum requires an extra processing step, slightly increasing the cost of the bath per sample and increasing the amount of time needed per sample. Nickel is also compatible with ENP and results in high fidelity features. However, nickel is a more expensive material and is stronger and harder than aluminum.

Table 5.1 Substrate Material Property and Cost Comparison

Material	625 Nickel (0.125" Plate)	6061 Aluminum (0.125" Plate)
Cost (per in^2)	$2.17	$0.25
Yield Strength (MPa)	414	241
Rockwell Hardness	60	50
Additional Plating Processing	No	Yes

Aluminum is easily oxidized when exposed to oxygen and a layer of aluminum oxide forms on the surface of the substrate. This layer inhibits the successful bonding of nickel ions to the surface of the aluminum. This can be overcome by using a zincate solution to chemically remove the oxidized surface layer while simultaneously applying a layer of zinc [15]. This is done by submerging an aluminum substrate in a zincate solution containing dissolved zinc ions and a sodium hydroxide salt solution. When the zinc surface is later exposed to the ENP solution, the zinc is dissolved and nickel plates onto non-oxidized aluminum [16].

To zincate an aluminum surface, per the Caswell protocol, this study combined 2 mL of the zincate solution concentrate with 8 mL DI water in a small sample dish to plate a 1” × 1” x 0.19” aluminum sample. The substrate was submerged in the zincate solution for approximately one minute, until the surface turned a dark grey color. The substrate was then rinsed with DI water before plating. Figure 5.4 shows a 1”×1” aluminum substrate that has been zincated. The sample was placed in a zincate solution such that only one half of the surface area was exposed to the zincate in an effort to save ENP solution in the following ENP steps, as ENP will only plate on zincated aluminum.

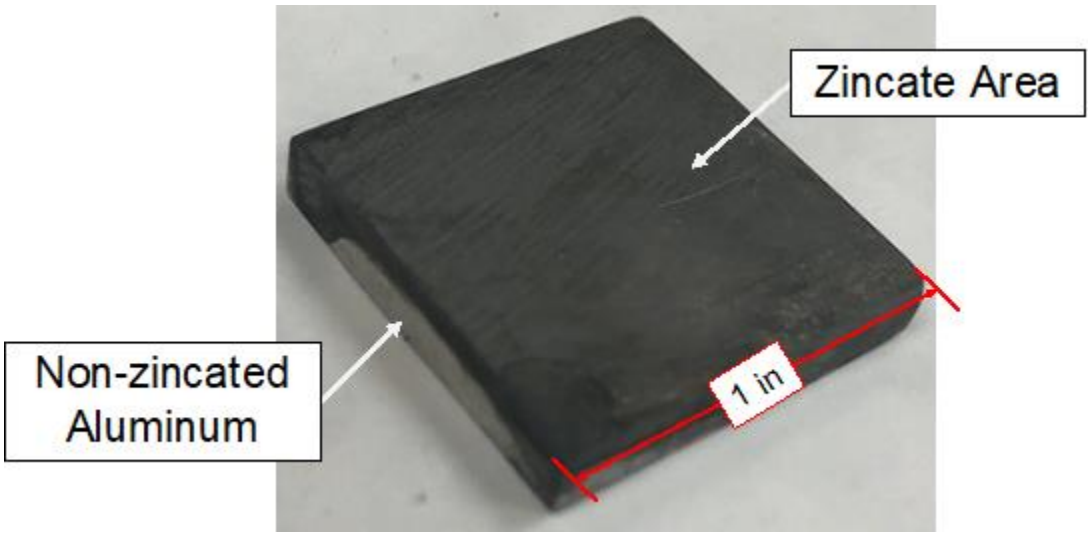

Figure 5.4 Zincated aluminum sample

Figure 5.5 shows a 1"×1" aluminum substrate exposed to ENP solution for 30 minutes; prior to ENP, the left half of the substrate was zincated while the right half was untreated. The surface that was zincated prior to ENP shows an even, uniform nickel plating, while the untreated surface shows splotchy, uneven deposition.

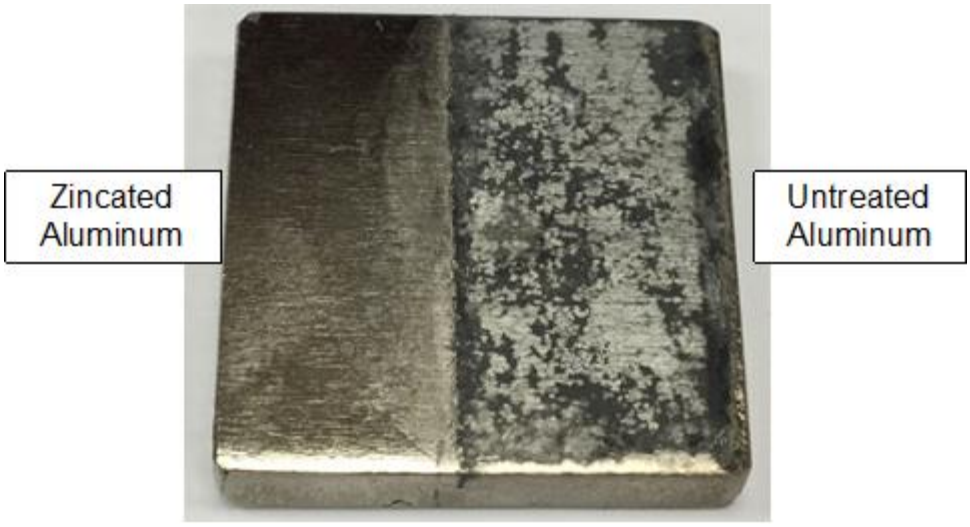

Figure 5.5 Effect of plating on zincated vs untreated aluminum surfaces

While the metal material was selected to promote nickel plating, the materials used in the mold—silicon wafers (University Wafer) and SU-8 3050 photoresist (MicroChem)—were chosen specifically because they do not readily plate with nickel during the ENP process. However, this study found that over time, debris in the bath or contaminants on the surface of the wafer could build up and cause the solution to plate on the SiO_2 surface of the wafer. To prevent this, a surface treatment was applied to the mold before use: the wafer was treated with trichlorosilane (Trichloro(1H,1H,2H,2H-perfluorooctyl)silane, Sigma Aldrich) to alleviate this effect. Exposure of silicon wafers to this chemical causes the surface to be superhydrophobic. To treat the surface, the wafer is placed in a vacuum

chamber with a few milliliters of the acid. When the pump is turned on, the acid vaporizes and deposits onto the surface of the wafer. After running the vacuum for 30 minutes, the wafer was removed from the vacuum chamber. This surface treatment rendered the silicon hydrophobic, which prevented nickel plating on the mold surface, even during hours-long ENP processes.

5.2 Assembly of Mold and Metal Plating Substrate

In order to generate the desired surface pattern during ENP, the silicon/SU-8 mold and metal substrate must be held in contact with each other during the entire process. If contact is lost, the ENP solution will reach areas between the SU-8 surface and the substrate, resulting in uneven metal feature heights or even loss of features, as shown in Figure 5.6 . To prevent this effect, a fixture was developed to hold the mold and plating substrate in place while providing uniform contact pressure to ensure that the SU-8 contacted the surface evenly.

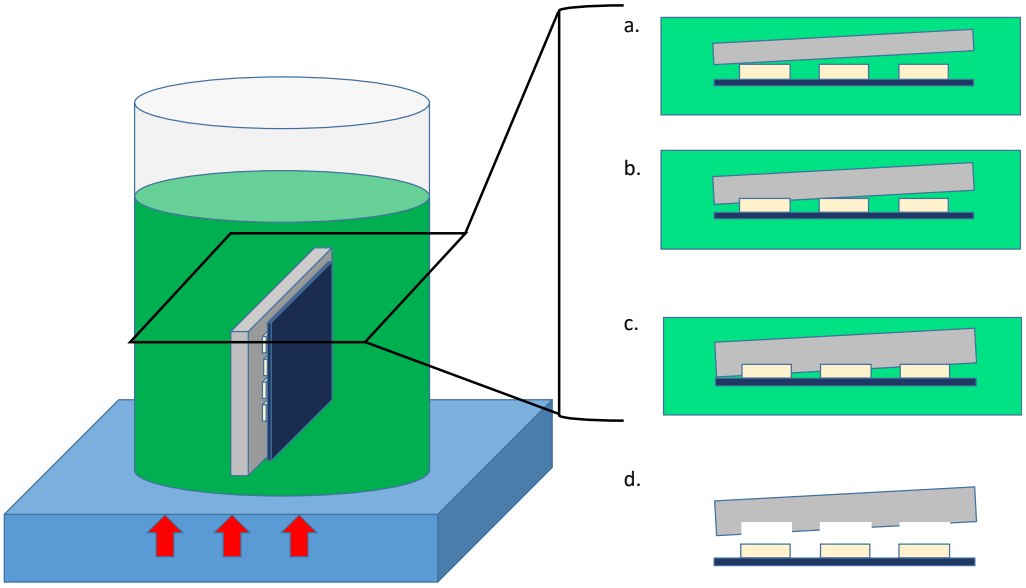

Figure 5.6 Results of uneven contact: a) initial uneven contact between metal and mold; b,c) metal deposits during ENP processing; d.) mold removed from substrate, feature height varies by location

Materials for the fixture were chosen such that they would not plate with nickel during the ENP process. This is especially important, because the concentration of nickel in the ENP solution is dependent on the plateable surface area. When plating a higher surface area, the nickel concentration decreases much more rapidly; therefore, to control the concentration of the nickel and catalyst in the bath, it was critical that the total plating area be highly controlled. By ensuring all components surrounding the substrate are nonreactive, the concentration of ENP solution during plating is predictable and easily maintained. The simplest way to ensure that it will not interact with the bath solution was to make all of the components of acrylic or other polymers, as shown in Figure 5.7.

Polypropylene chemical-resistant 10-32 bolts and nuts acquired from McMaster Carr. The acrylic plates were laser-cut from 10 mm thick sheet stock (McMaster Carr). The glass slides were Thermo Fisher Scientific standard 3 in x 2 in glass microscope slides.

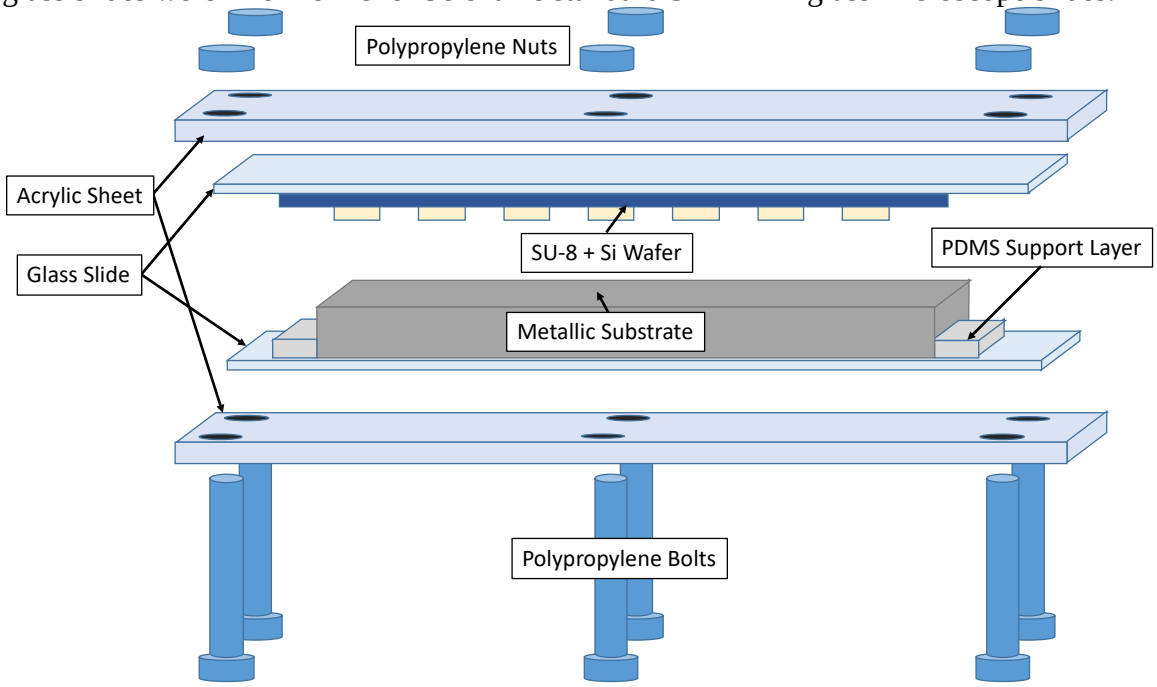

Figure 5.7 Exploded isotropic view of the mold-substrate assembly

Figure 5.8 includes geometric and material details of each component included in the contact apparatus assembly.

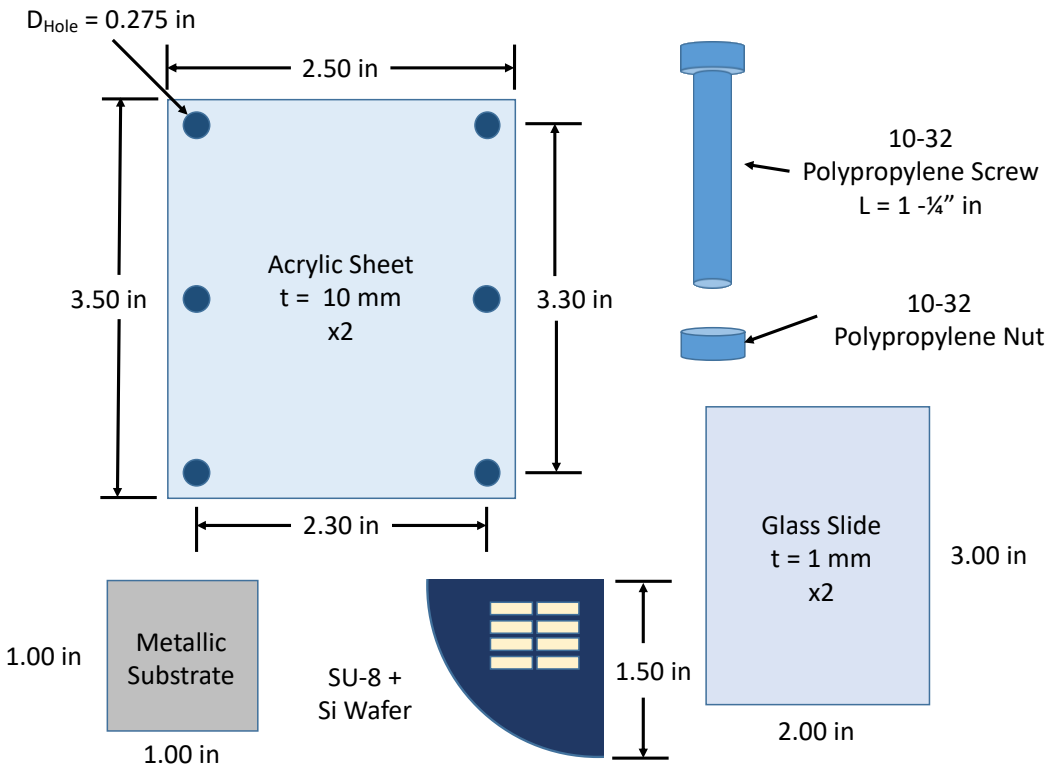

Figure 5.8 Geometric design details of the contact apparatus

Any movement of the substrate or mold early in the plating process will result in misalignment of the final features. The PDMS Support Layer shown in Figure 5.7 is a thin layer of polydimethylsiloxane (PDMS, Sylgard 184, Dow Chemical) cast on the glass in order to hold the substrate in place. PDMS was chosen because it can be easily removed after plating and does not readily plate with nickel during the ENP process. A picture of the PDMS layer, glass microscope slide and metal substrate are shown in Figure 5.9. Because each mold could only be used for one plating session, molds were adhered a the glass slide with super glue to prevent sliding while in the bath. Figure 5.10 shows the entire assembled contact apparatus.

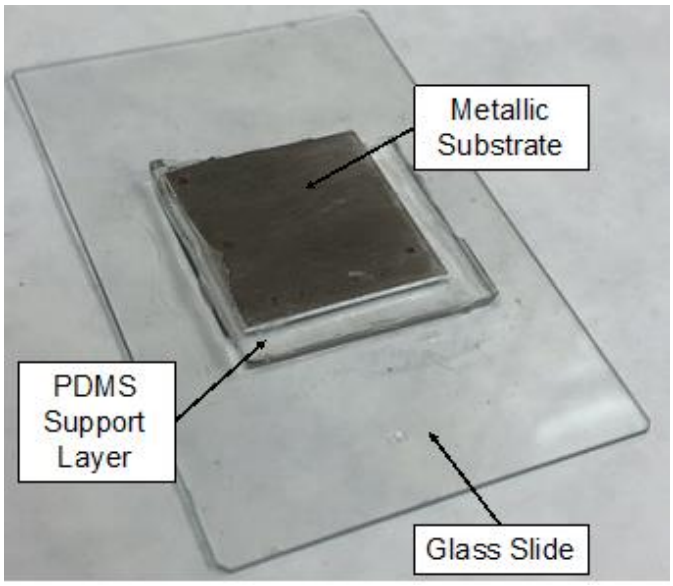

Figure 5.9 1" x 1" metal substrate adhered to glass microscope slide using PDMS

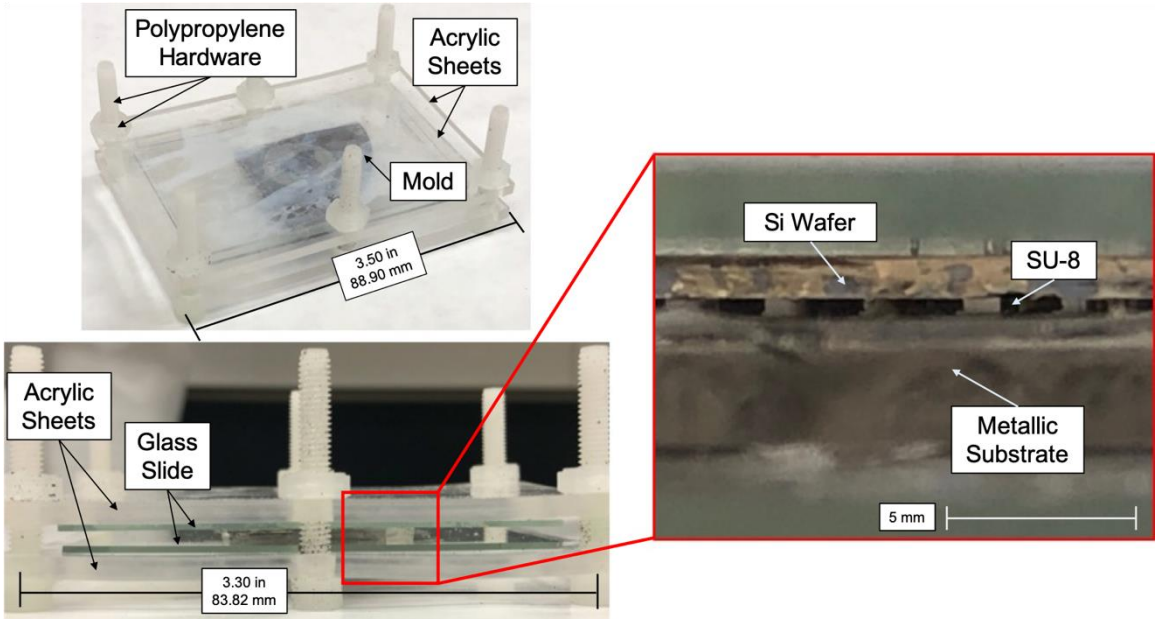

Figure 5.10 Assembled mold-substrate contact apparatus

5.3 Electroless Nickel Plating Protocol

Commercially available ENP plating materials were used throughout this experiment. All solutions were purchased from Caswell, Inc.; they were used as received and plated following the manufacturer's instructions. The Caswell products used in this study were Electroless Nickel Plating Part A, Part B, and Part C. When using an aluminum substrate, the Caswell zincate solution was also required (Figure 5.11).

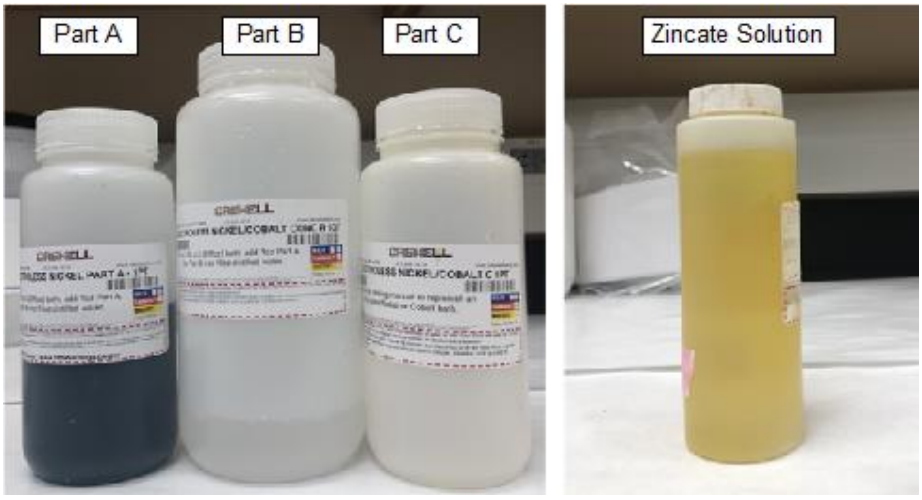

Figure 5.11 Caswell Plating ENP solution materials

Part A is 45% nickel (II) sulfate ($NiSO_4$) solution and provides the Ni^{+2} ion for deposition. Part B is 25% sodium hypophosphite ($NaPO_2H_2$) and 10% ammonium hydroxide (NH_3) to provide catalyst for ionizing the nickel sulfate and the surface of the metal substrate. Part C is 30% $NaPO_2H_2$ and 2% sodium hydroxide (NaOH) and is used to add catalyst into the bath as the system plates the substrate; this component is usually called a bath refresher. Additional materials that were necessary for plating included a hotplate with stirring capabilities, magnetic stir bar, a glass container large enough to hold the mold apparatus and enough solution to sufficiently submerge the sample, and a thermometer. The glass container used in this study, depending on the sample size, was a 500 mL or 1,000 mL beaker. The plating setup is shown in Figure 5.12.

Figure 5.12 ENP solution setup on hot plate under fume hood

Because ENP relies on a chemical reaction driven by heat, the process itself is temperature sensitive. Figure 5.13 shows how the solution temperature affects the plating or deposition rate [14]. The steep slope at higher temperatures shows that even a

relatively small reduction in temperature from 90°C (the temperature recommended by Caswell) will cause a relatively large reduction in plating rate. On the other hand, if the temperature of solution increases too close to boiling, the water in the solution will evaporate quickly, causing an increase in solute concentration in the plating solution. In order to minimize these problems, a thermometer and temperature controlled hotplate was used to monitor and control the temperature of the bath during plating.

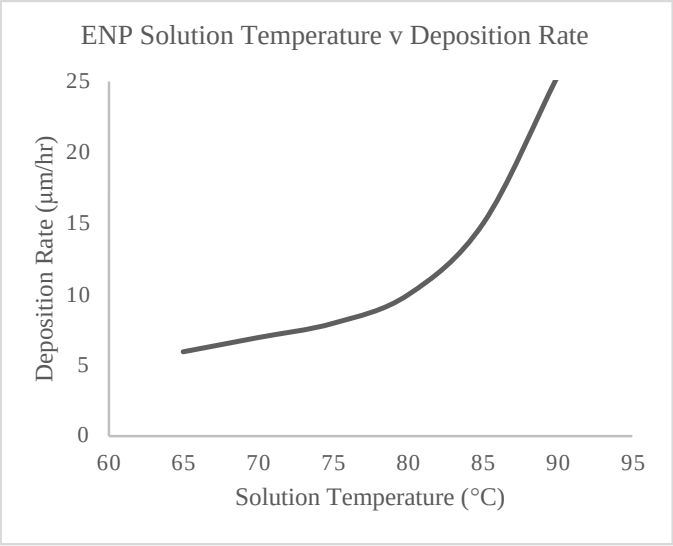

Figure 5.13 Solution Temperature vs Deposition Rate [10, 14]

The necessary concentration of nickel in the ENP solution, and therefore, the amount of each Caswell component required, is dependent on the total surface area being plated and the desired feature height. This system is designed to plate at a rate of 25.4 μm/hour when run at the optimized concentration and temperature. The amount of each component needed can be calculated as follows:

$$A \cdot t = V_{Ni} \tag{5.1}$$

Where A is the surface area of the plating substrate, in units of in^2, t is the thickness of the desired nickel layer (height of nickel features) in units of μm, and V_{Ni} is the total volume of deposited nickel, in units of $\text{in}^2 \cdot \mu\text{m}$. From there, the minimum necessary amount of each Part, per Caswell protocol, to achieve the required nickel and catalyst concentrations is calculated as:

$$\begin{aligned} V_{PartA} &= V_{Ni} \cdot 0.16\ \text{mL}/(\text{in}^2 \cdot \mu\text{m}) \\ V_{PartB} &= V_{Ni} \cdot 0.47\ \text{mL}/(\text{in}^2 \cdot \mu\text{m}) \\ V_{DIWater} &= V_{Ni} \cdot 2.48\ \text{mL}/(\text{in}^2 \cdot \mu\text{m}) \end{aligned} \tag{5.2}$$

For example, if a 1”×1” substrate was used and the desired feature height was 100 μm, the amount of each material required is:

$$\text{Part A} : 1\ \text{in}^2 \cdot 100\mu\text{m} \cdot 0.16\text{mL}/(\text{in}^2 \cdot \mu\text{m}) = 16\ \text{mL of Part A}$$

$$\text{Part B} : 1\ \text{in}^2 \cdot 100\mu\text{m} \cdot 0.47\text{mL}/(\text{in}^2 \cdot \mu\text{m}) = 47\ \text{mL of Part A}$$
$$\text{DI Water} : 1\ \text{in}^2 \cdot 100\mu\text{m} \cdot 2.48\text{mL}/(\text{in}^2 \cdot \mu\text{m}) = 248\ \text{mL of Part A}$$

In practice, if the minimum amount of required solution for a given sample was found to be less than the amount that would fully submerge the substrate, each component was scaled up in the ratio shown to generate the minimum volume required to submerge the substrate.

Due to the autocatalytic nature of the reaction, the bath must be maintained such that it always contains a minimum amount of the initial concentration of nickel and catalyst. Caswell recommended a concentration of 80% as the lower bound for a functioning ENP bath. If the concentration falls below 80%, the bath will decompose and will need to be remade. This is due to a combination of factors and interactions occurring in the bath, but in summary, if the free floating nickel ions reacts with other precipitates in the solution, the concentration of plateable ions drops rapidly, and no nickel will be able to plate on the substrate [14].

The nickel and catalyst concentrations were maintained by incrementally adding more Part A and Part C to ensure the solution concentrations remained at or greater than 80% of the initial concentrations. Thus, it is necessary to calculate the amount of time it takes to deplete 20% of the initial concentrations of the nickel and catalyst and replenish the solution every time the solution starts to become depleted.

For example: to deposit a nickel layer that was 100 μm thick on a 1 in^2 metal surface area, it would take 100 μm/(25.4 μm/hour) or just under 4 hours total, but 20% of the total concentration would be plated once 20 μm was deposited. It would take 20 μm/(25.4 μm/hour) or just over 45 minutes to plate 20% of the original available nickel. With a 4 hour plating time, the bath would need to be replenished every 45 minutes, or 4 times in total. The amount of each solution to be added each time can be calculated as a percent of the original volume; in the current example, 20% of the original volume of Part A would need to be added: 20%(Part A) = 20%(16 mL) = 3.10 mL every 45 minutes. Part C is used instead of Part B when replenishing the solution, but is added at similar concentrations: 20%(Part B) ≈ 20%(Part C) = 20%(47 mL) = 9.30 mL of Part C every 45 minutes.

Because the solution is maintained at a high temperature, water levels must also be maintained to make sure the substrate remains submerged in solution without compromising the concentrations of the nickel and catalyst. As the water in the solution evaporates, more water was added in small amounts throughout the plating process to bring the total fluid volume back up to the original amount. The DI water was added in these small increments to prevent extreme temperature or concentration changes that might occur with the additions of large batches of water.

Once the plating was complete, the plating contact apparatus was removed from the bath. The wafer and substrate were removed from the acrylic apparatus and placed in a freezer for at least 30 minutes, in order to make it easier to separate the mold and metal substrate.

5.4 ENP Experimental Results and Discussion

This section describes ENP experiments that were completed to provide proof-of-concept and to qualitatively evaluate the viability of this methodology as an microscale manufacturing technique for aluminum and nickel. In addition, some investigative experiments were run in an effort to categorize the rate of nickel deposition compared to the expected rate of deposition quoted by the ENP solution manufacturer, and whether agitation of the ENP bath played a role in this number. Finally, an effort was made to determine what effect, if any, the choice of base metal for plating had on the plating rate and final product. For the experiments detailed here, the SU-8/silicon mold feature heights were all 120 μm tall.

5.4.1 ENP on Zincated Aluminum

Two 1" x 1" x 0.19" polished aluminum blocks were zincated, assembled with SU-8/silicon molds, and then patterned using the ENP deposition process described in this chapter. The samples were plated for two hours: sample 1 was plated without any agitation of the ENP solution aside from nominal disruptions during refreshing the ENP bath. Sample 2 had constant agitation of the ENP solution provided by a magnetic stirring bar at 300 rpm. After the plating process, deposition was measured using a surface interferometer (Zygo Newview). Figure 5.14 shows the results of these experiments: a.) photographs of the plated substrates after the mold was removed, with clearly visible nickel features, b.) microscope images taken using the Zygo interferometer, c.) surface profile maps of a single feature on each sample, and d.) the 2D surface profile of the cross section line in b.) shown as a line connected by two triangles.

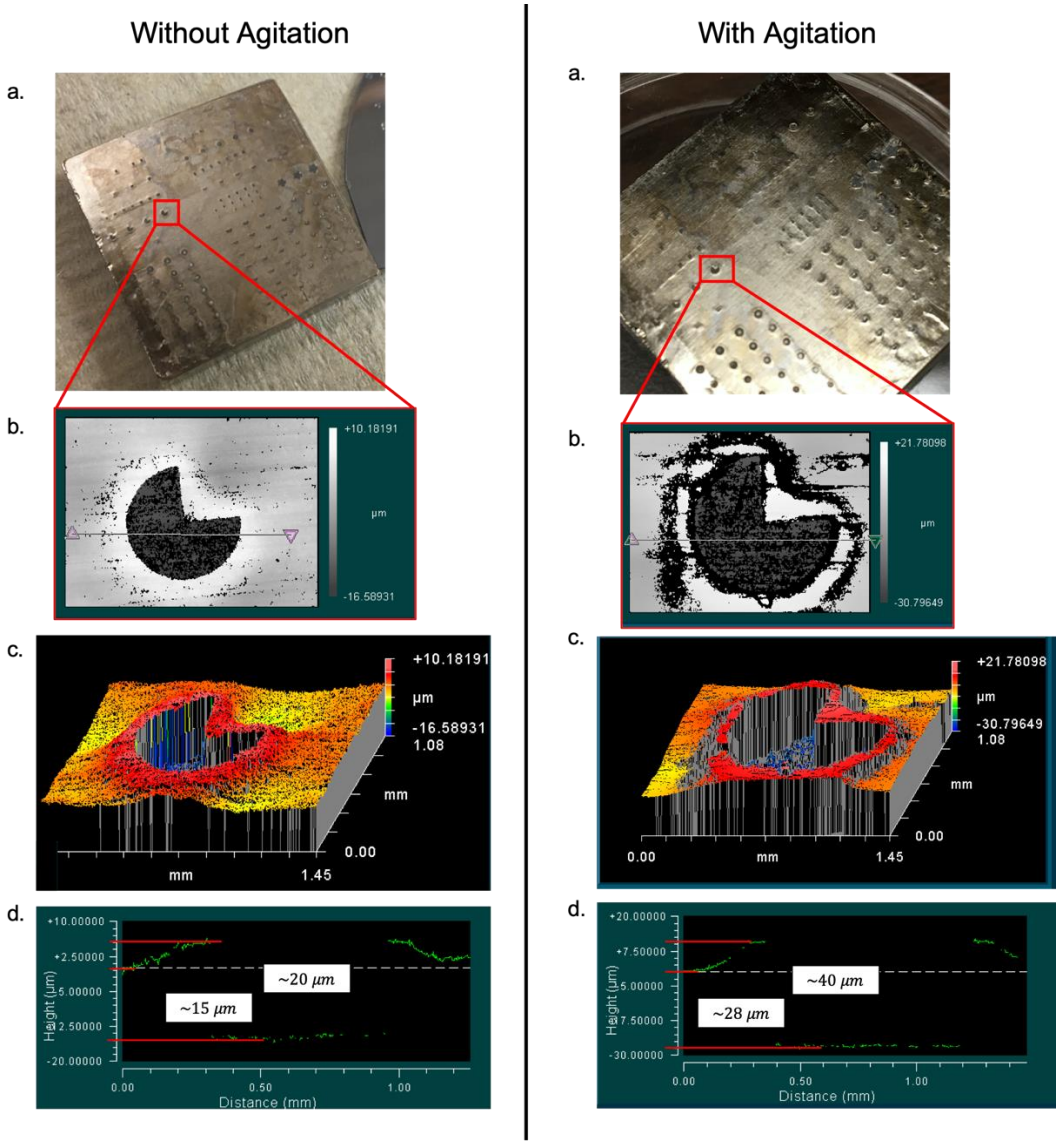

Figure 5.14 Aluminum substrate plated for two hours, without agitation (left) and with agitation (right)

Even with the naked eye, nickel patterns were visible on both samples after the deposition process was complete (Figure 5.14a). Using the data from the Zygo analysis, the nickel surface was measured to be thicker in general on the agitated sample: 28 µm versus 15 µm on the non-agitated sample), supporting the idea that agitation increases the ENP deposition rate in these samples. This is most likely caused by the agitation causing increased fluid flow between the mold and the sample, increasing the speed with which spent ENP liquid is removed from the surface and replaced with fresh solution. Examination of the Zygo results also show an area of raised material around the perimeter of the feature in both samples (Figure 5.14c,d). While it exists in both samples, it was taller in the agitated sample: 40 µm (or 12 µm above the flat nickel surface) in the agitated sample versus 20 µm (or 5 µm above the flat nickel surface) in the non-agitated sample. This raised region could be either indicative of local delamination of the deposited nickel during the removal of the mold, or local increased plating rate near the

mold features. After inspection under an optical microscope, no evidence of delamination was found (Figure 5.15), therefore it appears that there is local increased plating rate near the mold boundary.

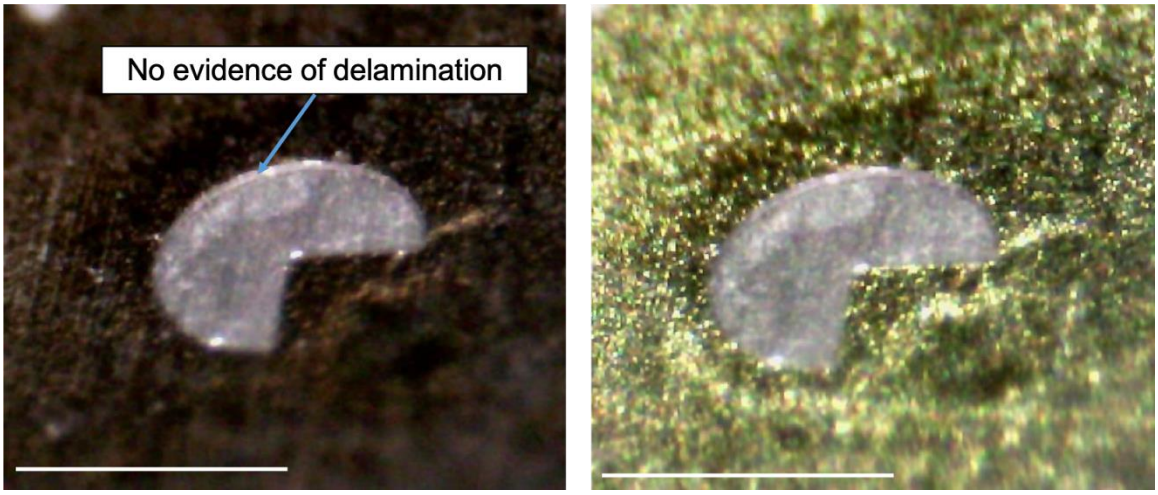

Figure 5.15 Raised feature edge in nickel-patterned aluminum sample. Scale bar = 0.65 mm

These results indicate that the plating rate for these samples is about 7.5 µm/hour for non-agitated solution and 14 µm/hour for the agitated sample. This implies that the use of agitation increases the plating rate by about 45%. However, this is still less than the published 25.4 µm/hour by the manufacturer. In addition, the ENP process appears to deposit material preferentially near sharp corners, causing the raised-edge effect seen in these results. This effect was more pronounced in the agitated case, although it is unclear whether this was due to the agitation itself, or simply that the raised-edge effect becomes more pronounced as a thicker layer of nickel is deposited.

5.4.2 ENP on Bulk Nickel

Four 1" x 1" x 0.0625" nickel samples were polished, assembled with SU-8/silicon molds and plated using the ENP process. Two samples were plated for two hours, while the other two nickel samples were plated for four hours. One sample from each time group was subjected to agitation via a magnetic stirring bar at 300 rpm, while the other was plated without agitation. Similar to the zincated aluminum samples, after deposition the samples were separated from their molds and measured using a Zygo 3D Optical Profilometer.

Figure 5.16 shows a low and high magnification microscope image taken of each plated sample. While all four samples showed evidence of micropattern deposition, the clarity of the pattern varied between samples, with the "2 hour + agitation" sample containing the most pristine set of features. Blurring of pattern, as evident in the "2 hour – agitation" sample is believed to have been caused by a loss of contact between the mold and the substrate, as illustrated by Figure 5.21. Additionally, as evident in the "4 hour – agitation," the poor feature resolution of the sample is believed to have been caused by a

layer of the plated features delaminating from the surface while the mold is removed from the surface of the substrate.

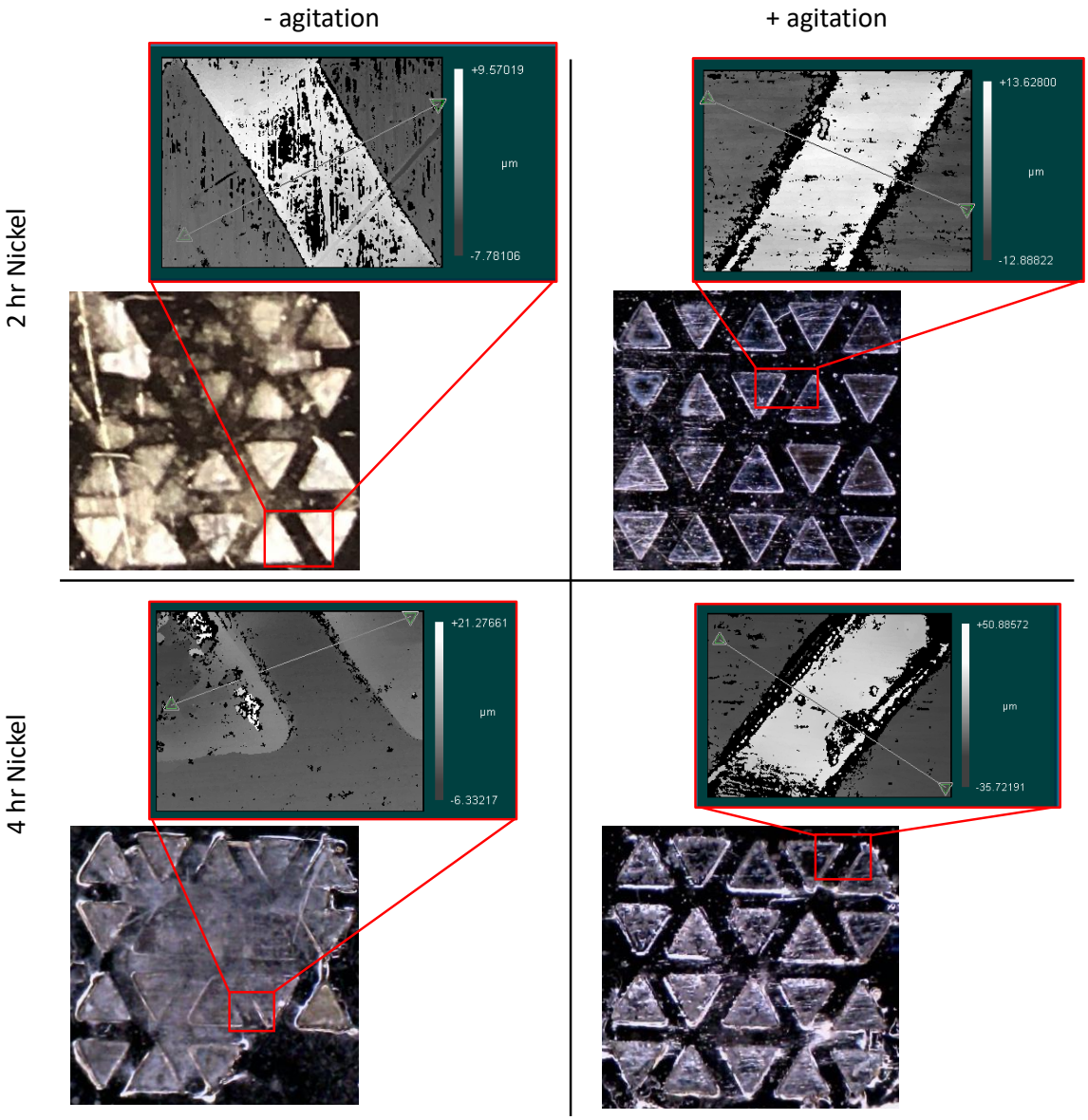

Figure 5.16 Nickel substrate, microscope image at region of interest

Figure 5.17 details the Zygo Microscope measurement of the surface profile at the cross section shown in Figure 5.16 (indicated as a white line between two samples) or each plated sample. While the "4 hour – agitation" sample may not accurately represent results, comparing the other three sample sets shows an increase in deposition rate in the presence of agitation (7 µm in "2 hour –agitation" sample versus 17 µm in "2 hour +agitation" sample). Additionally, comparing the two agitated samples shows what appears to be a linear increase in nickel height with plating time (17 µm at 2 hours versus 35 um at 4 hours). The "4 hour – agitation" sample shows that near the defect area, that

the plating height is inverted to the other samples. The cause of this is unknown but it is believed to be a combination of loss of contact between the mold and substrate and delamination.

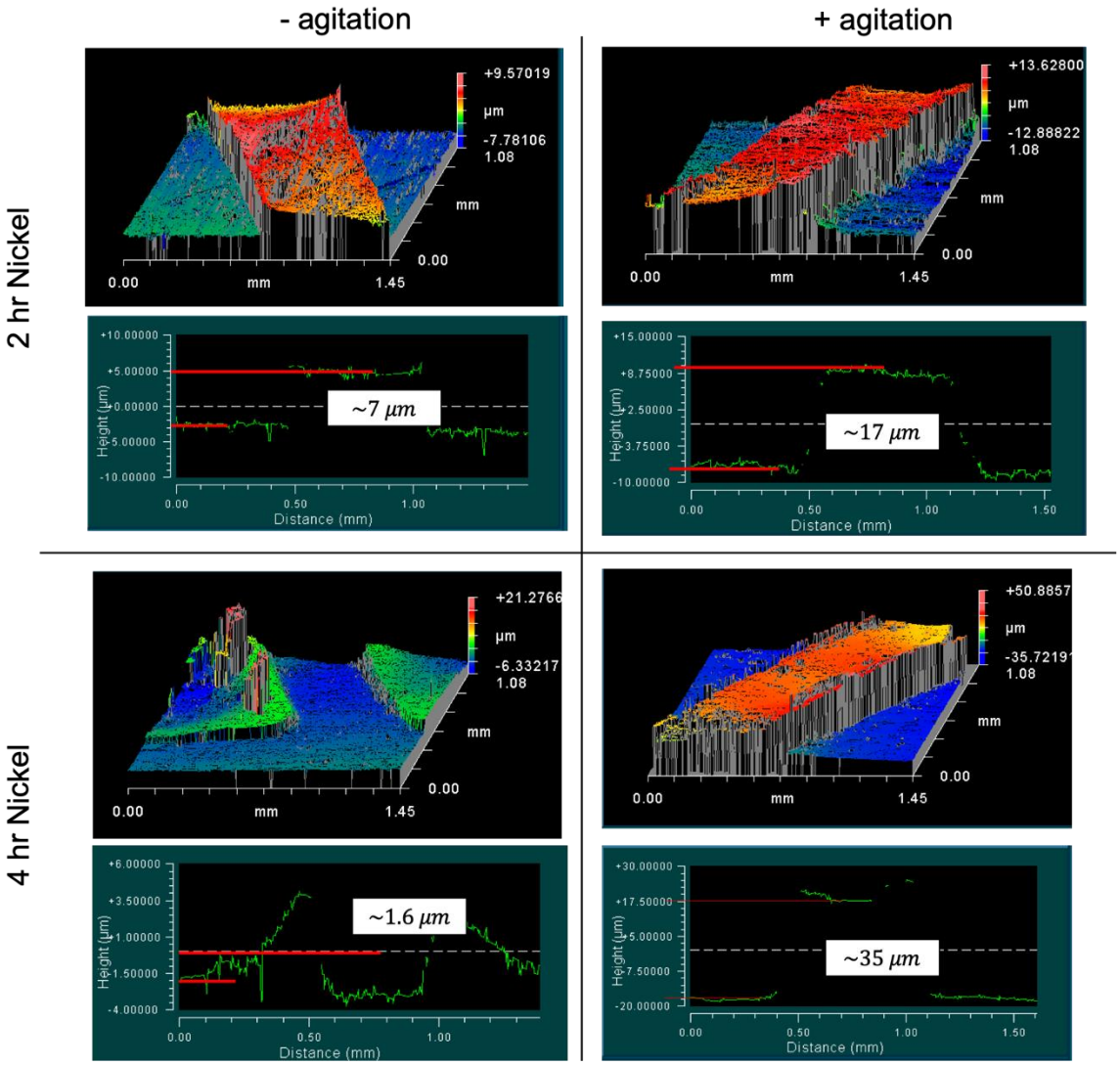

Figure 5.17 Nickel substrate, measured Zygo results from cross section

The expected geometry based on the Caswell published plating rate of 25 µm per hour is illustrated in Figure 5.18.

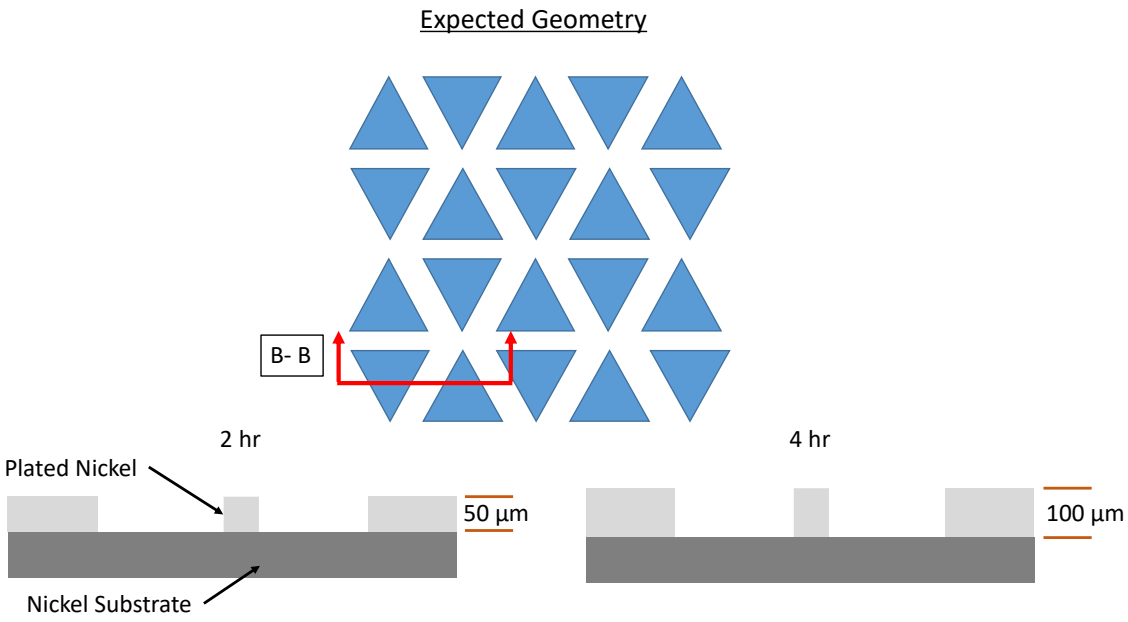

Figure 5.18 Expected plated geometry for nickel samples

Figure 5.19 summarizes the results of plating rate measurements between the two aluminum and four nickel samples. To obtain this data, 10-12 measurements were taken across the surface area of each substrate and used to calculate minimum, maximum, mean, and standard deviation values for nickel height on each surface. In these samples, agitation was shown to increase the mean plating rate by about 50%. For a 2-hour plating time, aluminum shows an average plating rate of 13 µm/hour for an agitated sample and 9 µm/hour for the non-agitated sample where nickel is found to have a plating rate of 7 µm/hour for the agitated sample and about a 2 µm/hour plating rate for the non-agitated sample. However, it should be noted that the difference in plating rates between materials may be due to using a different plating pattern in each set of experiments. Thus, the difference in feature density may have caused the difference between the experimental groups, rather than the base material.

The mean plating rate for micropatterned nickel in this work was found to be about 6 µm/hour. This is 76% less than the published plating rate of 25.4 µm/hour. However, note that the Caswell plating rate is based on open surface plating, meaning there are no issues with obstruction or diffusion of solution or gaseous products. This implies that the more space there is for solution and products to diffuse, the closer the plating rate should be to 25.4 µm/hour.

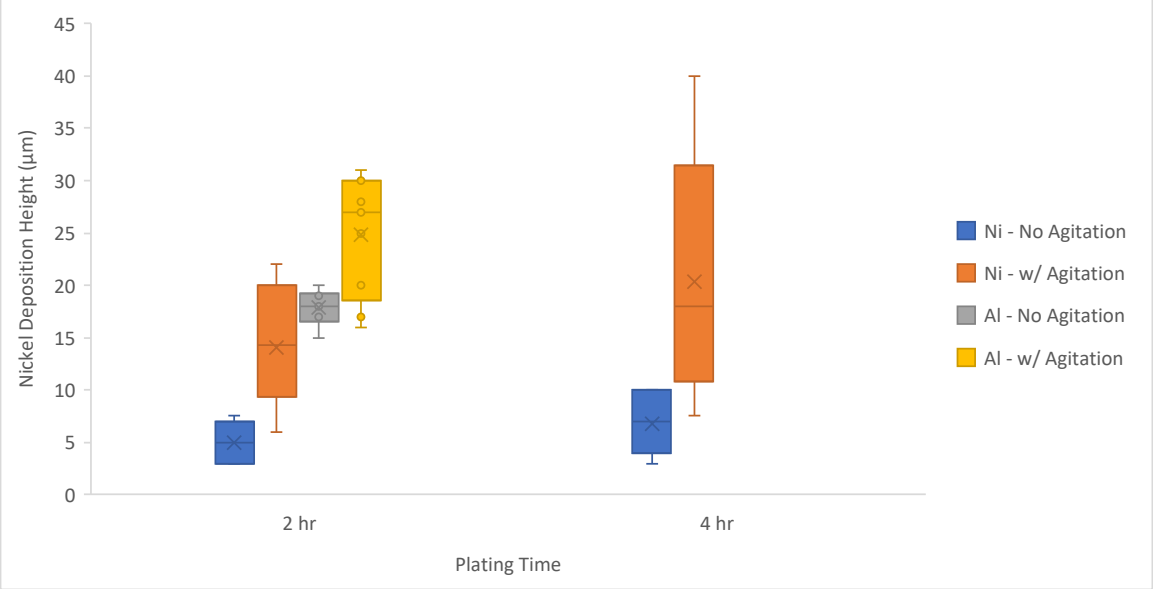

Figure 5.19 Plating height (µm) of nickel substrate across the surface of the sample

5.4.3 Uniformity and Defects

Heights of the nickel features on one of the aluminum sample with agitation was measured at nine separate locations on the surface, and this information was used to generate Figure 5.20, which shows the plating rate across the surface area of an aluminum substrate with a uniform plating pattern. This figure shows that the plating height varies across the total surface area, with a variability of about 10-15 µm. This variability could be due to pattern density, bubble trapping, or poor contact while plating.

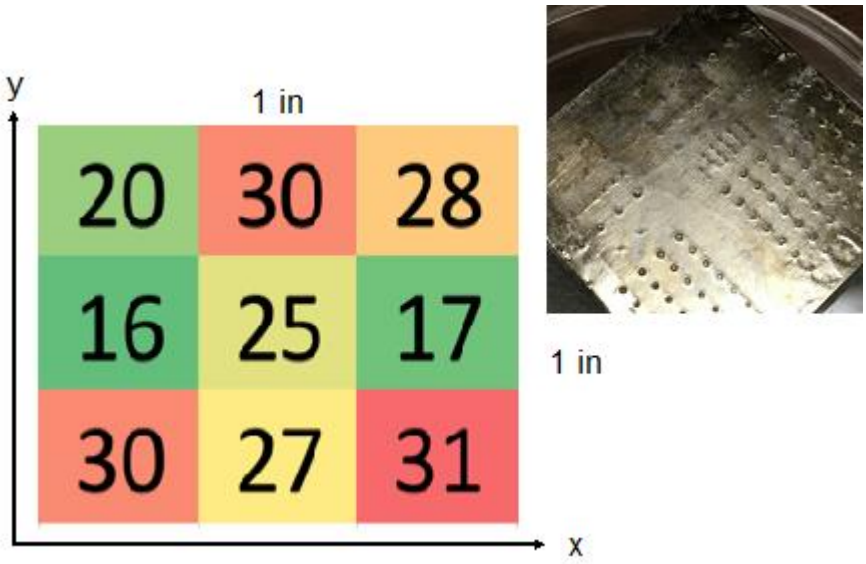

Figure 5.20 Plated height of small, distributed patterned features over substrate surface

In addition to the baseline variability observed during plating—like that shown in the previous sample—there were also some samples with contact issues that resulted in plated nickel between the mold and the substrate (i.e., the "4 hour – agitation" sample in the previous section). This loss of contact appears to have an interesting effect, where it actually produces the inverse of the desired geometry. Figure 5.21 shows how the loss of contact impacts the plating pattern: features on the right hand side of the sample demonstrate the desired geometry (recessed hexagonal wells surrounded by deposited nickel walls of ~10 µm height). However, the features on the left hand side show the exact opposite: slightly raised hexagonal posts that are 2-4 µm taller than the surrounding surfaces. While the exact cause of this is unknown, it is reasonable to speculate that a small gap separated the mold and base substrate in this range, and the same edge effect that caused raised geometry near corners in other samples caused nickel to selectively deposit more quickly in the resulting gap. This mechanism would be an interesting topic for future study.

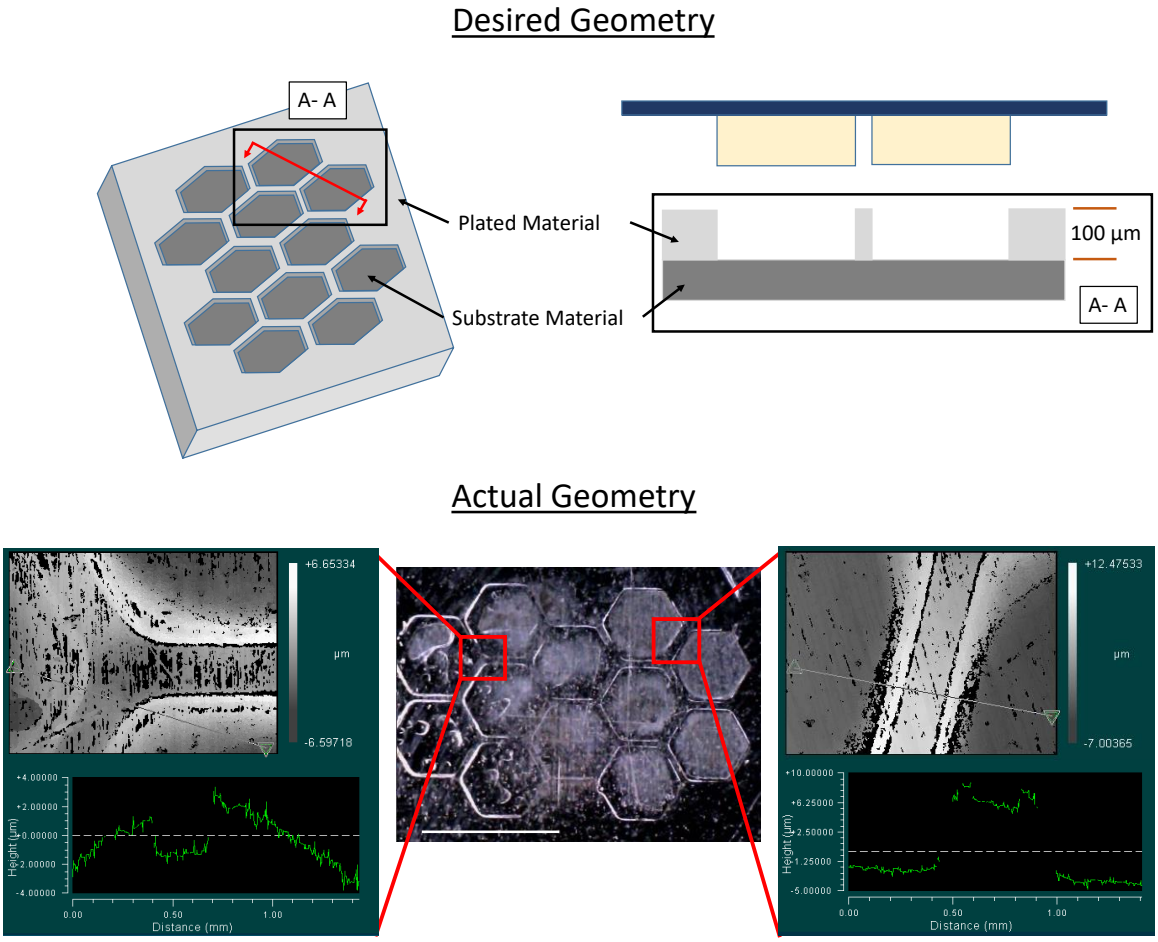

Figure 5.21 Effect of contact loss during ENP reaction, Scale bar = 3.73 mm

In addition to loss of contact, another defect that can occur with this method is the delamination of features. When plating is complete, the SU-8 mold is separated from the substrate, and in some cases, this would break newly plated features off of the surface.

This occurred more frequently with ENP samples on a zincated aluminum substrate, as shown in Figure 5.22. To alleviate this effect, the assembly was placed in a refrigerator or freezer prior to separation. The temperature decrease caused the metal to contract relative to the mold, and make separation of the two components easier.

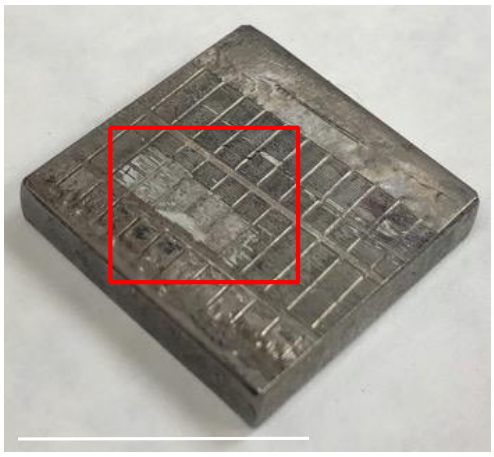

Figure 5.22 Feature delamination upon mold removal, Scale Bar = 25.4 mm

Chapter 6 Conclusions

This thesis describes the development of a microscale manufacturing protocol to fabricate metal features that fall in a size scale between standard machining capabilities and photolithography-based microfabrication. In particular, a method was developed for making SU-8/silicon molds (Chapter 3), creating molds with tapered geometry (Chapter 4) and demonstrating proof-of-concept creation of microscale metal features using ENP deposition (Chapter 5). The combined results from these experiments show that this approach shows promise and could be a viable metal micropatterning process with further development and an improved experimental setup.

The goal of this study was to develop 250-300 μm micropatterned nickel features. To achieve this, it required generating an SU-8 mold with similar feature heights that when pressed against a metal surface and placed in an ENP solution, the mold would guide the nickel deposition, resulting in a metal inverse pattern of the mold. 250-300 μm tall SU-8 features were successfully demonstrated by performing multiple spin coating and prebaking steps. Prior to spinning the layer of the desired features, a thin foundation layer was spun, exposed, and post-baked, but not developed, to provide a higher adhesion strength for the thin contact area to the wafer. Once the feature layers were spun, following exposure, gradually bringing the wafer to post-bake temperature at increments of 10ºC to help reduce internal stresses caused by the temperature change. Developing the wafer with a sonicator helped dissolved the SU-8 faster.

Once the mold was created, it was secured to a metallic substrate and submerged in ENP solution and allowed to plate for 10 hours. Based on published plating rates for the ENP chemicals used in this thesis, this was expected to result in the desired nickel thickness of 250um. However, in these experiments a plating rate of 10 um/hour was observed, compared to the 25 um/hour published rate. This is likely due to the slower diffusion of the gaseous byproduct from the autocatalytic reaction. Additionally, it was found that molds would delaminate or deform after extended periods in the ENP solution. A practical upper limit for this method is about 8 hours of exposure. Thus, the maximum plated feature height achievable by the protocol is theoretically around 80 um.

One area of development could be exploring the use of other mold materials besides SU-8/silicon. This particular combination was somewhat time intensive to produce and because the molds degraded during the ENP process, each mold could only be used once. Exploring materials like a PDMS “daughter” mold cast from a SU-8/silicon mold rather than using the SU-8/silicon mold directly would decrease the cost per mold and increase the life of the SU-8/silicon wafer. A PDMS mold would be much more easily fabricated, the “parent” wafer mold could be reused multiple times to cast multiple PDMS molds. The mold would also be more flexible which would aid in the mold removal step, but in preliminary trials, the material softness also distorted the pattern more easily.

Another factor to investigate is to determine if there are ways to mitigate the reaction limiting effects that happen during ENP. The decreased plating speed compared to the rate quoted by the ENP solution manufacturer was likely due to the small gap between

the mold and substrate, which limited diffusion of products and reactants in this gap. Agitation helped with this process, refreshing the ENP solution locally and dislodging the bubbles formed on the substrate surface. The use of a vacuum or reducing the adhesion force between the gas bubbles and the plating surface could further increase the flow of solution to the substrate surface. The gas diffusion could also be added by optimizing mold geometry—for instance, by increasing the feature height on the molds, or by adding macroscale channels in either the substrate or mold to allow for even more solution flow during the ENP process.

Appendix A
Procedure for creating SU-8/silicon molds with 250 μm tall vertical-sidewall features

Materials needed

- SU-8 3050
- 3" silicon wafer
- Plastic dish and cover to place wafer in once protocol is complete
- SU-8 Developer
- 3.5" or larger glass dish that can hold wafer and developer to submerge wafer (x2)
- Isopropyl alcohol (IPA) or ethanol
- Access to UV filtered light clean room with:
    - All relevant personal protective and contaminant protective wear such as face masks, nitrile gloves, plastic coveralls, hair net, etc.
    - Compressed air or nitrogen
    - Spin coater (may come with multiple chuck sizes, confirm that the size being used is compatible with wafer size before adding SU-8 to surface)
    - Hot plate or oven that can reach 95°C
    - Sonicator
    - Small metal tongs
    - Container for disposed developer
    - Ventilation system/fume hood station for development
    - Mask aligner and UV exposure system

I. Liquid SU-8 deposition and prebake for foundation layer

1. Clean wafer by rinsing with IPA; blow dry with nitrogen or compressed air
2. Place wafer on chuck, pour enough SU-8 3050 into center of wafer to cover approximately 1/3 of the wafer area. Be careful not to introduce bubbles during pouring by not moving the stream of SU-8 around
3. Spin wafer at 3000 rpm for 1 minute with 5 second ramp up and ramp down.
4. Prebake wafer on hotplate for 10 minutes at 95°C. No ramp up or ramp down is necessary for this layer.
5. Allow to cool to room temperature before placing in mask aligner

II. UV exposure for foundation layer

1. Using a laser cutter, a large piece of acrylic of thickness roughly equal to a typical glass-chrome photomask was cut to the dimensions shown in Figure A1.0.1 below. Aluminum foil was covered and adhered on this piece of acrylic's top surface (surface facing the UV bulb) and cut around the 1.75" x 2.0" cut-out to create a make-shift photomask. This uncovered area will act as the exposure area for the foundation layer. The dimensions are oversized relative to the pattern to allow for some positional error.

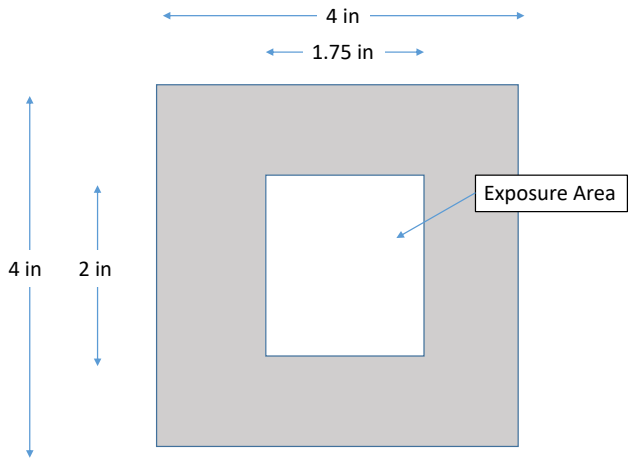

Figure A1.0.1 Acrylic Photomask Dimensions

2. Clean photomask using IPA and blow dry with compressed air or nitrogen before placing in mask aligner
3. Using the mask aligner photomask holder (typically by vacuum channels), place the aluminum foil side to the holder, then setting it in place under the bulb
4. Place the prebaked and cooled wafer on the wafer platform and check that soft contact where there is acrylic is achieved
5. Expose the SU-8 to 200 mJ/cm^2 (times may vary by mask aligner, confirm bulb power before exposure with luminometer)
6. Release contact, remove wafer, and place on hotplate at 95°C for 7 minutes.
7. DO NOT DEVELOP, total area of cured and uncured SU-8 is important for following spin steps.

III. Liquid SU-8 deposition and prebake first layer of patterned features

1. Before first spin step, adjust hotplate to 65°C (unless multiple hotplates are available, in which case have hotplate available at 65°C. Using a digital hotplate is the easiest, but you should confirm temperature is correct with a thermometer
2. Using the wafer from steps I. and II., place wafer in spin coater and pour enough SU-8 3050 into center of wafer to cover approximately 1/3 of the wafer area.
3. Spin at 1000 rpm for 1 minute with 5 second ramp up and ramp down
4. Quickly remove wafer from the spin coater and place on hotplate at 65°C.
5. The prebake and post-bake steps for the multi-layer SU-8 are critical. For the prebake step, continue with the following temperature ramp up procedure:
   65°C for 5 min
   75°C for 10 min
   85°C for 10 min
   95°C for 30 min
   85°C for 10 min
   75°C for 10 min
   65°C for 5 min
6. Allow to cool to room temperature
7. Repeat steps 3 and 4 of this section to deposit 2nd layer of SU-8 3050

8. Prebake with the following ramp up procedure:
    65°C for 5 min
    75°C for 10 min
    85°C for 10 min
    95°C for 60 min
    85°C for 10 min
    75°C for 10 min
    65°C for 5 min
9. Allow to cool to room temperature
10. Repeat steps 3 and 4 of this section to deposit 3rd layer of SU-8 3050
11. Prebake with the following ramp up procedure:
    65°C for 5 min
    75°C for 10 min
    85°C for 10 min
    95°C for 150 min
    85°C for 10 min
    75°C for 10 min
    65°C for 5 min
12. Allow to cool to room temperature

IV. UV Exposure for multi-spin layers

1. Clean patterned photomask using IPA and blow dry with compressed air or nitrogen, then place in mask aligner
2. BE SURE TO LOWER THE MASK CONTACT because if you had soft contact with the previous exposure, if you try to bring to contact with the current setting, it will crush the SU-8 causing deformation of the final features (if accidentally applied too much pressure before exposure, the wafer can be baked for about 10 minutes at 95°C with some ramp up and down to reset the SU-8).
3. Expose the wafer to 500 mJ/cm^2
4. Post-bake to the following temperature ramp up procedure
    65°C for 5 min
    75°C for 10 min
    85°C for 10 min
    95°C for 40 min
    85°C for 10 min
    75°C for 10 min
    65°C for 5 min
5. Allow to cool to room temperature before developing. Check that features are visible after exposure and post-bake.

V. Development

1. With so much SU-8 on the surface of the wafer, multiple development steps may be necessary, but always check the wafer during development as the developer can begin to dissolve the exposed SU-8 after prolonged exposure. Development:
    i. Move wafer, glass dish, developer, and sonicator under the vent hood
    ii. Fill sonicator to water line with water

iii. Place wafer in glass tray/dish and pour SU-8 developer until wafer is completely submerged, but be careful to not overfill the dish so that it doesn't spill while moving the dish around.
iv. Place glass dish with wafer and developer in sonicator such that it floats on top of the water
v. Turn on sonicator with 5 minute timer – continuously check in on the wafer that uncured SU-8 is dissolving; make sure to perform this step in a functioning fume hood, as the developer is quite toxic.
vi. Continue for about 4 rounds of 5 minute intervals and check on wafer, if uncured SU-8 remains on the surface, by this time, the developer may become saturated with dissolved SU-8 and will not be able to continue to dissolve any more.
vii. With the metal tongs, remove the wafer from the developer and place in additional glass dish
viii. Discard saturated developer to proper disposal container
ix. Repeat steps iii. – vi. until all uncured SU-8 is dissolved

2. Once the SU-8 has been developed, immediately rinse with IPA
   (If any white material forms when exposed to IPA, there is likely trace amounts of undeveloped SU-8 on the wafer, repeat development steps until when rinsing with IPA does not produce white by product)
3. Do not dry with compressed air or nitrogen
4. Rinse surface with ethanol. As ethanol has lower surface tension than IPA, this aids in mitigating effects of capillary force between channel walls. Air dry wafer with compressed nitrogen or filtered air.

Bibliography

1. Ohring, M., *Thin-Film Evaporation Processes*, in *Materials Science of Thin Films*. 2001, Elsevier Science & Technology: ProQuest Ebook. p. 95-144.
2. Bunshah, R.F., Schramm, R.J. , *Alumina deposition by activated reactive evaporation.* Thin Film Solids, 1977. **40**.
3. Wasa, K., *Basic Process of Sputtering Deposition* in *Handbook of Sputter Deposition Technology*, I.K.a.H.K. Kiyotaka Wasa, Editor. 1992, Elsevier: The Boulevard, Langford Lane, Kidlington, Oxford OX5 1GB, UK. p. 297-352.
4. M R Rashidian Vaziri, F Hajiesmaeilbaigi, M H Maleki, *Microscopic description of the thermalization process during pulsed laser deposition of aluminium in the presence of argon background gas.* Journal of Applied Physics, 2010. **43**.
5. Gillespie, L.K., *Micro Milling*, in *Design for Advanced Manufacturing: Technologies and Processes*. 2017, McGraw-Hill Education. p. 12.
6. Yunn-Shiuan Liao, Shun-Tong Chen, Chang-Sheng Lin, Tzung-Jen Chuang, *Fabrication of high aspect ratio microstructure arrays by micro reverse wire-EDM.* Journal of Micromechanics and Microengineering, 2005. **15**: p. 1547-1555.
7. Gillespie, L.K., *Micro Electrical Discharge Machining*, in *Design for Advanced Manufacturing: Technologies and Processes*. 2017, McGraw-Hill Education. p. 10.
8. Microchem. *SU-8 3000 : Permanent Epoxy Negative Photoresist*. Available from: https://engineering.dartmouth.edu/microeng/processing/lithography/SU83000DataSheet.pdf.
9. del Campo, A., Greiner, C., *SU-8: a photoresist for high-aspect-ratio and 3D submicron lithography.* Journal of Micromechanics and Microengineering, 2007. **17**: p. R81-R95.
10. Becnel, C.J., *Ultra deep SU-8 manufacturing and characterization for MEMS applications*, in *Department of Mechanical Engineering*. 2004, Louisiana State University. p. 83.
11. C. Beuret , G.-A. Racine , J. Gobet , R. Luthier , N.F. de Rooij, *Microfabrication of 3D multidirectional inclined structures by UV lithography and electroplating*. 1994, Proceedings IEEE Micro Electro Mechanical Systems An Investigation of Micro Structures, Sensors, Actuators, Machines and Robotic Systems: Oiso, Japan. p. pp. 81-85.
12. Pearlstein, F., *Electroless Plating*, in *Modern Electroplating 3rd ed. (F.A. Lowenheim, ed.)*. 1974, John Wiley & Sons: New York, NY.
13. Baudrand, D., *Adhesion of Electroless Nickel Deposits to Aluminum Alloys*, in *Products Finishing*. 1999.
14. Glenn O. Mallory, Juan B. Hajdu, *The Fundamental Aspects of Electroless Nickel Plating*, in *Electroless Plating*. 1990, William Andrew.
15. Zipperian, D.C., *Physical And Chemical Characteristics Of The Zincate Immersion Process For Aluminum And Aluminum Alloys*, in *Material Science and Engineering*. 1987, University of Arizona.
16. Vangelova, T., , Lubnin, E. , Armyanov, S., *Auger-Spectroscopic Investigation Of The Deposition Of Nickel-Phosphorus Layers On An Aluminum Alloy.* Soviet Electrochemistry (A Translation of Elektrokhimiya), 1984. **20**: p. 1527-1531.

Vita

Lorli Smith graduated from the University of Kentucky with a Bachelor's of Science in Mechanical Engineering in 2016. Following her bachelor's, she began work as a structural analysis engineer at Belcan Engineering until 2020 and since early 2020 has been a structural engineer at Sierra Nevada Corporation.